DIPLOMARBEIT

Titel der Diplomarbeit

ER-associated degradation of glycoproteins in a glucosylation-deficient
Chinese hamster fibroblast cell line

angestrebter akademischer Grad

Magister/Magistra der Naturwissenschaften (Mag. rer.nat)

Verfasserin / Verfasser:	Johanna Levy
Matrikel-Nummer:	0217591
Studienrichtung /Studienzweig (lt. Studienblatt):	A490 Diplomstudium Molekulare Biologie UniStG
Betreuerin / Betreuer:	Ao. Univ.-Prof. DI Dr. N. Erwin Ivessa

Wien, am 12.03.2010

Acknowledgment

I would like to express my gratitude to everyone who gave me the possibility to complete this thesis. First and foremost I want to thank my adviser Mr. N. Erwin Ivessa, who was most helpful and supportive throughout the entire time.

Moreover, I want to thank my family and friends who believe in me and are there whenever I need them.

Table of contents

1. Aims of research:

The endoplasmic reticulum (ER) is a key organelle in the secretion pathway involved in the synthesis of both proteins and lipids destined for multiple sites within and outside the cell (Lavoie and Paiement, 2006). It is responsible for correct folding and delivery of proteins of the secretory pathway. Thus, it contains sophisticated protein proof reading and elimination mechanisms (Kostova and Wolf, 2003). The mechanisms guaranteeing the integrity and fidelity of secretory proteins in the ER are termed ER quality control (QC). If a protein fails to reach its correctly folded native conformation it does not pass the final QC checkpoints. Then the protein is not transported to its final destination in the cell and instead is eventually degraded by a process termed ER-associated degradation (ERAD). During ERAD, non-native proteins are retro-translocated from the ER into the cytosol where they are ubiquitylated and thereafter degraded by proteasomes (Ellgaard and Helenius, 2003).

The aim of this study was to investigate the degradation of a specific glycoprotein by the ERAD pathway in wild type and glycosylation-deficient cells. The N-glycosylated model glycoproteins used in this study were RI_{332}, a truncated version of ribophorin I (RI) and RI_{332}-6HA, an HA-tagged version of RI_{332} (Kitzmueller et al., 2003). Ribophorin I is a transmembrane glycoprotein found abundantly in the ER. It is part of the oligosaccharyltransferase (OST), a multisubunit protein complex carrying out a critical step in asparagine-linked glycosylation (ALG) of proteins (Kelleher and Gilmore, 2006). The shortened, soluble versions of RI, RI_{332} and the tagged RI_{332}-6HA, substrates for the ERAD-ubiquitin-proteasome pathway, have been used in previous studies of ERAD (Ermonval et al., 2001; Kitzmueller et al., 2003) and thus represent ideal model substrates for investigation of protein degradation. The experimental model cells used in this study were G3 and QC hamster fibroblasts permanently expressing RI_{332} or RI_{332}-6HA. G3 fibroblasts represent the wild type and thus the control cells, whereas QC fibroblasts are glycosylation deficient mutants that produce N-glycosylated proteins lacking glucosylation (Flores-Diaz et al.,1998; 2004). As glucosylation is critical for the interaction of glycoproteins with the calnexin/calreticulin cycle, this cell model should allow a better understanding of the role of this pathway in ERAD.

Furthermore, experiments using inhibitors of proteasomal degradation such as ZLLL and inhibitors of N-glycan processing such as castanospermine, dMM and kifunensine were performed. The aim was to study their influence on glycoprotein processing and degradation in the ER based on observations in preceding studies in HeLa cells (Kitzmueller et al., 2003).

2. Introduction:

2.1. Quality control (QC):

In order to maintain the integrity of a cell an important feature is quality control (QC). Quality control mechanisms exist for synthesis of DNA, RNA and proteins so as to keep accumulations of errors in macromolecules in the cell low. Concerning proteins, QC occurs at the level of translation, folding and assembly. If a protein fails to reach its correctly folded native conformation it does not pass the final QC checkpoints. Then the protein is not transported to its final destination in the cell and is eventually degraded. Discrimination of native and non-native protein conformations is carried out by various sensor molecules including molecular chaperones and enzymes that covalently tag misfolded proteins which lead to recognition by the folding and degradation machinery (Ellgaard and Helenius, 2003). Proteins destined for secretion, the plasma membrane or the cell surface are translocated from the cytosol into the endoplasmic reticulum. The ER is the organelle responsible for proper folding and delivery of these proteins and contains sophisticated proofreading and degradation mechanisms. Failure of protein quality control leads to disease and cell death (Kostova and Wolf, 2003).

2.1.1. Primary and secondary quality control in the ER:

On the one hand, protein QC works at a general level termed primary QC that is applied to all proteins based on common structural and biophysical structures. On the other hand, secondary QC acts at a specific level for selected proteins.

Primary QC is dependent on the recognition of features such as exposure of hydrophobic regions, unpaired cysteine residues and the tendency to aggregate. The molecular chaperons and folding sensors carrying out this mechanism are found abundantely in the ER (Ellgaard and Helenius, 2003). Binding Protein (BiP), glucose-regulated protein (GRP) 94, protein disulphide isomerase (PDI), the lectins calnexin (CNX), calreticulin (CRT) and ER degradation enhancing 1, 2-mannosidase-like protein (EDEM) as well as UDP-glucose:glycoprotein glycosyltransferase (UGGT) and ERp57 are among the most important workers in the secretory protein factory (Ellgaard and Helenius, 2003; Anelli and Sitia, 2008).

Specific proteins and protein families have to undergo further proofreading mechanisms in order to be secreted (Ellgaard and Helenius, 2003). Once the proteins are folded they are no longer substrate to primary QC and thus they can leave the ER through ER exit sites and for the Golgi complex. The factors of secondary QC act on folded proteins and late folding intermediates and effect maturation, assembly, folding and transport (Ellgaard et al., 1999). They can be assigned to three different groups. The "outfitters" establish or maintain a

secretion-competent conformation of the travelling protein, the "escorts" have a similar function but accompany their substrates to the Golgi and the "guides" provide signals for intracellular transport (Herrmann et al., 1999). Accessory proteins include ERGIC-53, p24 family, receptor-associated protein (RAP) as well as egasyn and carboxyl esterase (Ellgaard et al., 1999). Secondary QC is often cell-type dependent and frequently involved in the regulation of ER retention and export (Ellgaard and Helenius, 2003).

2.2. The endoplasmic reticulum:

The endoplasmic reticulum is an organelle that forms a network of tubules, vesicles and cisternae within eukaryotic cells. It is surrounded by a single membrane that separates the ER lumen from the cytosol. The ER lumen is extracytosolic and thus equivalent to the extracellular space. Therefore, the ER provides an environment optimized for protein folding and maturation and several cotranslational and post-translational modifications of proteins can take place that do not occur in the cytosol. These modifications include disulphide-bond formation, signal-peptide cleavage, N-linked glycosylation and glycophosphatidylinositol (GPI)-anchor addition (Ellgaard and Helenius, 2003).

There are two forms of the ER. The smooth ER is the site of lipid and membrane synthesis and completely lacks bound ribosomes. The cytoplasmic surface of the rough ER is studded with ribosomes and represents the site of protein synthesis.

Approximately one-third of all proteins in eukaryotes are targeted to the secretory pathway. The first compartment encountered by this diverse substrate ensemble is the ER (Ghaemmaghami et al., 2003; Kanapin et al., 2003). Secretory proteins are translocated into the ER in an unfolded state via an aqueous channel, the Sec61 translocon complex (Ruddock and Molinary, 2006). Once in the ER lumen the proteins are properly folded, assembled and modified by a large array of ER chaperones and enzymes (Kostova and Wolf, 2003). One major modification of many secretory proteins is called N-glycosylation and involves binding of a preformed oligosaccharide to the substrate protein carried out by the oligosaccharyltransferase (OST) complex (Kelleher and Gilmore, 2005). Proteins are allowed to exit the ER and enter the secretory pathway only when they are properly folded and modified (Ellgaard et al., 1999). To ensure correct folding several QC as well as degradation mechanisms take place in the ER such as unfolded protein response (UPR), calnexin/calreticulin cycle and ER-associated degradation (ERAD) (Kostova and Wolf, 2003). Native proteins enter vesicles at the ER exit sites and traffic through the ER-Golgi intermediate compartment (ERGIC) to the Golgi complex (Ellgaard and Helenius, 2003).

2.2.1. N-glycosylation and glycoprotein processing:

Asparagine-linked glycosylation is one of the most common protein modification reactions in eukaryotic cells (Kelleher and Gilmore, 2005) and represents a highly conserved mechanism in evolution (Yuki et al., 2005). N-glycosylation is unique to proteins targeted for the secretory pathway (Anelli and Sitia, 2008) and involves binding of a preformed oligosaccharide to asparagine side chains in the sequence Asn-X-Ser/Thr, where X is any amino acid other than proline (Khalkhall and Marshall, 1975). The luminal enzyme oligosaccharyltransferase (OST) scans the nascent protein entering the ER lumen for the required consensus sequences and mediates the attachment of pre-assembled, triantennary core glycan composed of two N-acetylglucosamine, nine mannose and three glucose residues (see figure 1, Ruddock and Molinary, 2006).
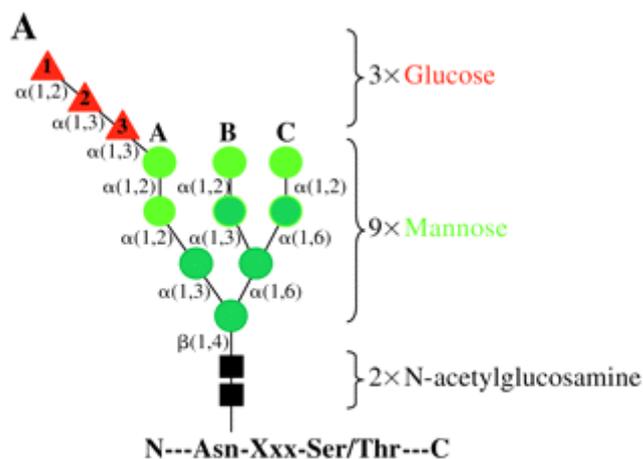
Figure 1 Core glycans added on protein nascent chains. (A) The complete oligosaccharide is composed of two *N*-acetylglucosamine residues (black squares), nine mannose residues (green circles), and three glucose residues (red triangles). Linkages are shown and the three N-glycan branches are labeled A, B and C (Ruddock and Molinary, 2006).

N-glycans contribute to the hydrophilicity of the unfolded, nascent proteins (Ruddock and Molinary, 2006) and are progressively trimmed by resident enzymes of the secretory pathway (Anelli and Sitia, 2008). In the ER and in the early secretory pathway, the repertoire of oligosaccharide structures is still small and the glycans play an important role in protein folding, oligomerization, quality control, sorting, and transport. In the Golgi complex, the

glycans acquire more complex structures and a new set of functions that the sugars display in the mature proteins (Helenius and Aebi, 2001).

In mammalian cells, the pre-formed oligosaccharide starts to be synthesized on the cytosolic surface of the ER. Sugars are added, one by one, to dolicholphosphate. When two N-acetylglucosamines and five mannoses have been added the oligosaccharide precursor is flipped to the luminal side of the ER where four more mannoses and three glucoses are added. The resulting core oligosaccharide is ready to be attached to the asparagine residues of a nascent protein by oligosaccharyltransferase (see figure 2, Helenius and Aebi, 2001).
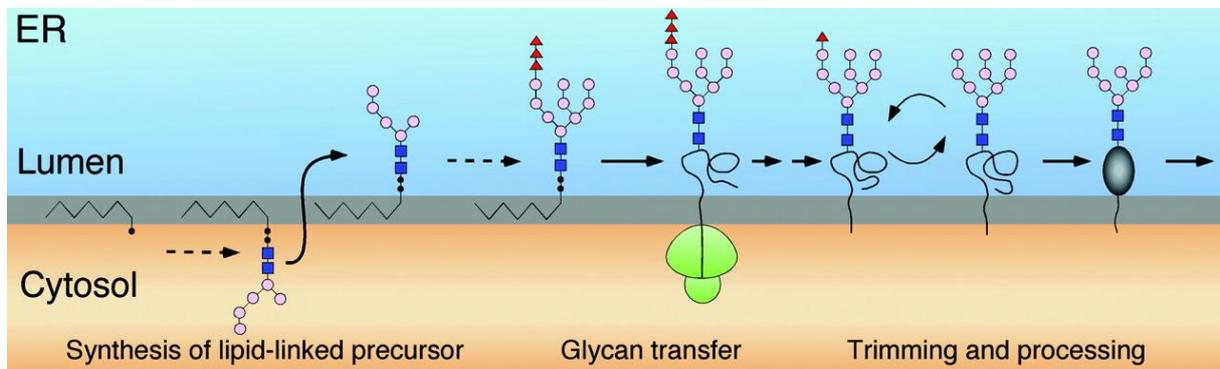
Figure 2 Synthesis of the lipid-linked precursor followed by transfer of the glycan to a nascent growing polypeptide chain (catalyzed by OST, green). Trimming and processing of the glycan by ER resident enzymes. When the protein has folded (gray oval) it is transported to the Golgi complex where further modification of the glycan takes place (Helenius and Aebi, 2001).

2.3. The calnexin/calreticulin cycle:

The calnexin/calreticulin (CNX/CRT) cycle (see figure 3) represents a well-characterized primary QC system in the ER. It is responsible for supporting folding of glycoproteins, retaining non-native glycoproteins in the ER until they have reached their folded conformation, and targeting terminally misfolded glycoproteins for degradation (Ellgaard and Helenius, 2003).
After transfer of the preformed glycan (Glc3Man9GlcNAc2) to asparagines residues of a nascent protein by OST the enzymes glucosidase I and II sequentially remove the three glucose residues attached to the A branch. Then the folding sensor UDP-

glucose:glycoprotein glucosyltransferase (UGGT) refits a glucose residue to N-glycans close to misfolded regions (Anelli and Sitia, 2008; Taylor et al., 2004). Calnexin and calreticulin specifically bind monoglycosylated glycoproteins and retain misfolded substrates in the ER, preventing their aggregation and promoting oxidative folding via association with the protein disulphide isomerase-like protein ERp57 (Anelli and Sitia, 2008; Ellgaard et al, 2001; Frickel et al., 2002; Russell et al., 2004; Taylor et al., 2004).

Glucosidase II removes the terminal glucose and dissociates the substrate from calnexin/calreticulin. Subsequently, the substrate undergoes novel inspection by UGGT and is exposed to, dependent on its folding state, either a novel round in the calnexin/calreticulin cycle, further transported along the secretory pathway or degraded.

Terminally misfolded proteins are substrates of ER-associated degradation (ERAD). Trimming of the terminal B branch mannoses inhibits glucose re-addition and thus the substrate is no longer able to associate with calreticulin/calnexin (Anelli and Sitia, 2008). Several enzymes are involved in targeting non-native proteins to ERAD including ER α1, 2- mannosidases and ER degradation-enhancing 1, 2-mannosidase-like proteins, namely the EDEMs 1-3. It has been shown that α1, 2- mannosidase I plays a crucial role in removing terminal mannoses but recent findings suggest that EDEMs which have been thought to serve as receptors for mannose trimmed glycoproteins may participate as well in the trimming process. Initially it was suggested that removal of a single mannose residue was sufficient for a glycoprotein to enter ERAD (Lederkremer, 2009). Indeed it was found that ERAD substrates are processed to M6 and M5, which means that most or all α1, 2 linked mannose residues are removed (Avezov et al., 2007).
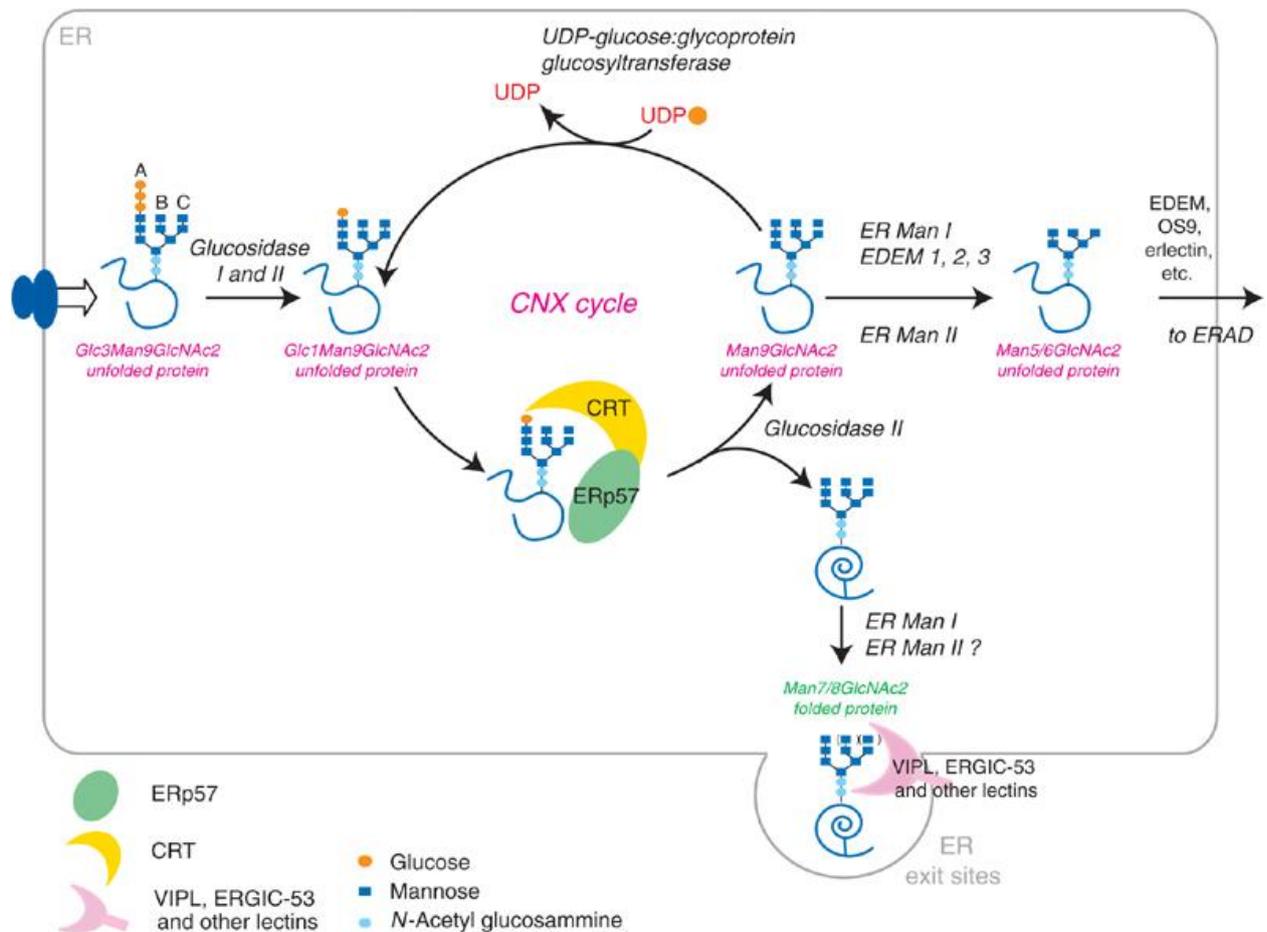
Figure 3 The CNX/CRT cycle (Anelli and Sitia, 2008)

2.4. Enzymes involved in processing of secretory proteins:

2.4.1. Oligosaccharyltransferase:

Asparagine-linked glycosylation (ALG) in eukaryotic cells is carried out by the oligosaccharyltranferase (OST) complex. OST catalyses the en bloc transfer of a preformed oligosaccharide onto asparagines residues of nascent proteins entering the lumen of the ER (see 2.2.1.). OST is a hetero-oligomeric protein complex consisting of seven subunits in mammals: ribophorin I, DAD1, N33/IAP, OST4, STT3A/STT3B, Ost48, and ribophorin II.

N-Linked glycosylation is temporally coupled to the protein translocation reaction and occurs as, or immediately after, the polypeptide is synthesized. In order to coordinate protein translocation and glycosylation, OST is localized adjacent to the protein translocation channel (Kelleher and Gilmore, 2006).

Diseases that affect glycoprotein biogenesis are called congenital disorders of glycosylation (CDG). They have a broad range of clinical phenotypes and affect nearly every organ system. Eighteen different types of CDGs have been defined genetically (Freeze and Aebi, 2005).

2.4.2. Trimming enzymes glucosidase I and II, ER α1, 2- mannosidase I:

Subsequently to ALG, glucosidase I, a type II membrane protein with a lumenal hydrolytic domain, rapidly removes the outermost of the three glucose moieties (Stigliano et al., 2009; Helenius et al., 2005). Glucosidase II is responsible for removing the middle glucose (cleavage I) and represents a soluble ER-resident heterodimer composed of two tightly but noncovalently bound α and β chains (GIIα and GIIβ) (Trombetta et al., 1996, 2001).The resulting monoglycosylated glycan allows the entry of the nascent protein into the calnexin/calreticulin cycle. Release of the substrate from the chaperones calnexin/ calreticulin is enabled by a second cleavage of glucosidase II which removes the remaining glucose. Properly folded proteins are able to leave the ER, whereas insufficiently folded proteins are re-glucosylated by UGGT and thus re-enter the calnexin/calreticulin cycle.
In recent studies it has been suggested that GII plays a regulatory role controlling the entrance of glycoproteins into CNX/CRT cycles. However, this putative function has to undergo extensive studies (Parodi and Caramelo, 2008).
ER α1, 2- mannosidase I plays a crucial role in targeting terminally misfolded proteins for ERAD cleaving the terminal mannose of the B branch (Helenius et al., 2005). Recently, it has been proposed that ERAD substrates are further processed to Man6 or Man5 (Avezov et al., 2007) and additional ER α1, 2- mannosidases as well as EDEMs participate in this process too (Lederkremer, 2009).
It has been shown that removal of mannose is slower than that of glucose by GI and GII. Thus, "mannose removal time clock" regulated disposal has been suggested. Irreparably misfolded glycoproteins staying in the ER for a relatively long period are demannosylated and targeted to degradation (Parodi and Caramelo, 2008).

2.4.3. UDP-glucose:glycoprotein glucosyltransferase:

UDP-glucose: glycoprotein glucosyltransferase (UGGT) is a soluble protein of the ER that consists of a large (80%) N-terminal folding sensor domain and a smaller (20%) catalytic C-terminal domain (Arnold et al., 2000). After trimming of the innermost glucose residue by glucosidase II, UGGT adds back a glucose moiety to N-glycans positioned near misfolded regions of the protein. Thus, UGGT acts as a folding sensor and produces monoglucosylated glycans that interact with calnexin or calreticulin (Taylor et al., 2004; Anelli and Sitia, 2008).

UGGT senses protein conformations as it recognizes hydrophobic amino acid patches exposed in molten globule-like conformers. Furthermore, UGGT glucosylates glycoproteins of not fully assembled oligomeric complexes because it recognizes hydrophobic surfaces exposed as a consequence of the absence of subunit components (Sousa and Parodi, 1995; Caramelo et al., 2003).

2.4.4. Calnexin and Calreticulin:

Nascent glycoproteins after trimming by GI and GII or re-addition of a glucose moiety by UGGT are substrates of the calnexin/ calreticulin cycle. Calnexin (CNX) and calreticulin (CRT) are related proteins that comprise an ER chaperone system that ensures the proper folding and quality control of newly synthesized glycoproteins. Their specificity for glycoproteins is determined by a lectin site that recognizes the oligosaccharide structure $Glc_1Man_9GlcNAc_2$. In addition, calnexin and calreticulin possess binding sites for ATP, Ca^{2+}, non-native polypeptides and ERp57, an enzyme that catalyzes disulfide bond formation, reduction and isomerization. Calnexin is a 90 kDa type I ER membrane protein, calreticulin represents its soluble homologue of 60kDa that is localized in the ER lumen by a C-terminal KDEL sequence (Williams, 2006). Of the glycoproteins associating with the chaperones some interact with only one of them whereas others bind both either simultaneously or sequentially (Helenius et al., 1997). The decision whether to bind CNX or CRT has been shown to be related to the number and location of the glycosylation sites of the substrate (Harris et al., 1998; Hebert et al., 1997), as well as the different topologies of CNX and CRT (Danilczyk et al., 2000; Wada et al., 1995).

Since GI and GII play important roles in targeting nascent proteins into the CNX/CRT cycle, experiments with glucosidase-deficient cell lines, cells with CNX or CRT deficiency as well as studies with inhibitors such as castanospermine (CST) of these enzymes have been performed to find out more about this pathway.
The more rapid folding observed in models of CRT or CRT deficiency, as well as the appearance of misfolded, aggregated, or disulfide cross-linked species, suggest that these chaperones normally delay folding, help suppress the formation of aggregates and promote correct disulfide-bond formation. Additional phenotypes frequently associated with CNX/CRT deficiency or CST treatment include more rapid export of non-native glycoproteins from the ER as well as their increased degradation (Williams, 2006).

2.4.5. ERp57:

Cysteine (Cys) represents an amino acid that is found more often than other residues in functionally important regions of proteins. Some of the functions include formation of structural disulfide bonds, metal binding, targeting proteins to the membranes, and various catalytic functions (Marino and Gladishev, 2008). Enzymes catalyzing the reduction, oxidation and isomerization of disulfide bonds are known as protein disulfide isomerases (PDI). ERp57 is one of the members of this protein family.

It contains four thioredoxin-like motifs, abb'a', where the a and a' domains contain catalytic CGHC motifs and the b and b' domains are non-catalytic (Maattanen, 2006). ERp57 interacts with the ER lectins calreticulin and calnexin primarily through its b' domain and to some extent through its positively charged C-terminus and thereby promotes the oxidative folding of newly synthesized glycoproteins (Ellgaard et al., 2004). The N-terminal cysteine residue of the CGHC motif forms mixed disulfides with substrate proteins during oxidation and isomerization reactions (Williams, 2006).
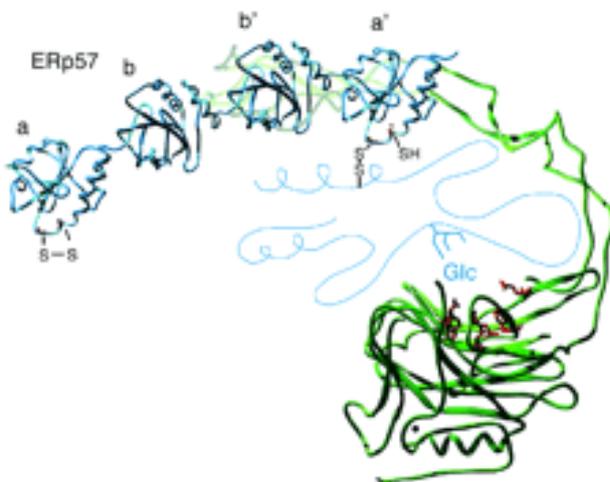
Figure 4 Model for the interaction of a folding glycoprotein with ERp57 and calnexin. Calnexin (green) is shown associated with a hypothetical model of ERp57 (blue) drawn on the basis of the NMR structure of the PDI `a' domain (Kemmink et al., 1996). The four domains of ERp57 are indicated: a, b, b', a'. A folding glycoprotein (thin blue line) may enter the cavity between the arm and globular domains interacting both with the lectin site as well as a polypeptide-binding site. The two CGHC active sites of ERp57 (red) are well-placed to catalyze disulfide-bond formation, reduction or isomerization (Williams, 2006).

2.5. ERAD:

Most proteins that misfold or fail to assemble properly leave the calnexin/calreticulin cycle and are targeted for degradation by ER-associated degradation (ERAD). This mechanism can be divided into several steps (see figure 5): protein recognition, protein targeting, retrotranslocation to the cytosol and ubiquitylation followed by degradation by the 26S proteasome (Williams, 2006; Vembar and Brodsky, 2008).
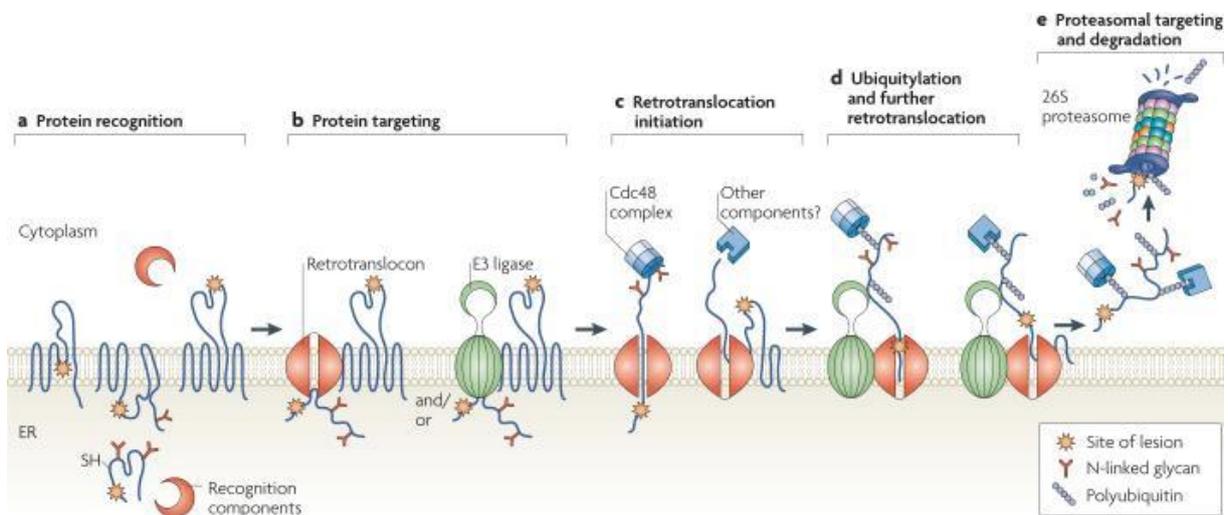
Figure 5 A step-by-step illustration of endoplasmic reticulum-associated degradation (Vembar and Brodsky, 2008)

Protein recognition:
Only correctly folded and processed glycoproteins can leave the ER and proceed along the secretory pathway. If an error is found proteins are degraded via the ERAD pathway. It still remains elusive for most ERAD substrates how the discrimination between native and non-native glycoproteins is made. As mentioned before, UGGT plays an important role as a folding sensor re-glucosylating glycoproteins and therefore targeting them to the calnexin/calreticulin cycle. Furthermore, it is not sure whether ERAD requires trimming of a specific number of mannoses and it still has to be investigated how factors such as calnexin / calreticulin, BiP, PDI and UGGT inteact with the ERAD pathway. However, it has been suggested that a large percentage of native proteins undergo ERAD as well (Varga et al., 2004, Vembar and Brodsky, 2008).

<u>Protein targeting:</u>

Since proteins targeted for ERAD might not be passed between different recognition and targeting complexes, protein recognition and targeting can become indistinguishable (Vembar and Brodsky, 2008). Two types of factors involved in recognition and targeting of aberrant proteins for the ERAD pathway have been identified. In mammals, EDEM1 and its homologues EDEM2 and EDEM3 and Htm1p/Mnl1p in yeast have been detected. However, it remains unclear whether the EDEMs exhibit substrate specifity, whether all three homologues possess mannosidase activity and whether binding to a distinct mannose-trimmed protein species is essential for substrate selection (Vembar and Brodsky, 2008).

The second type of lectin-like molecule discovered is Yos9p in yeast and OS-9 and XTP3-B/ERlectin in mammals. These molecules are believed to participate in glycan trimming and further in degradation of misfolded proteins, whereas the exact mechanism and nature of the glycan degradation signals that they recognize remains unclear (Yoshida and Tanaka, 2009).

Yeast Yos9 was suggested to exhibit chaperone-like activity involved in ERAD by binding to misfolded substrates. It was also discovered that Yos9 forms stable complexes with BiP and binds to Hrd1, possibly regulating the selectivity of the ubiquitin ligase for misfolded substrates (Vembar and Brodsky, 2008; Buschhorn et al., 2004; Gauss et al., 2006).

For OS9, interaction with GRP94 and the mammalian HRD1complex has been shown (Christianson et al., 2008). Concerning XTP3-B, different suggestions for its role have been made. Altogether, it will be important to determine whether members of the Yos9 family exhibit diverse substrate specificities, and what the relative contributions are between lectin-mediated binding and the observed chaperone-like activity (Vembar and Brodsky, 2008).

<u>Retrotranslocation and ubiquitylation:</u>

Prior to their degradation, nearly all ERAD substrates have to be ubiquitylated by a machinery that requires the action of an E1 ubiquitin-activating enzyme, E2 ubiquitin-conjugating enzymes and E3 ubiquitin ligases. Given that the catalytic sites of these factors are located in the cytoplasm substrates targeted for ERAD have to be retrotranslocated to the cytosol. The exact mechanism of this step remains unknown. However, it was shown that ubiquitylation is mandatory for most ERAD substrates (Nakatsukasa and Brodsky, 2008).

Several studies suggest that Sec61, the major component of the translocation channel importing polypeptides into the ER might serve as the retrotranslocon in ERAD as well. Nevertheless, other factors involved in retrotranslocation have been identified including Hrd1

and Doa10 in yeast and gp78 in mammals that are believed to function as both retrotranslocon channels and E3 ligases. Furthermore, Der1 in yeast and one of its homologues in mammals, Derlin1 have been proposed to be involved in degradation and /or retrotranslocation (Nakatsukasa and Brodsky, 2008; Vembar and Brodsky, 2008).

Proteasome degradation:

After ERAD substrates have been polyubiquitylated and retrotranslocated a series of ubiquitin-binding proteins escort the modified substrates from the ER to the proteasome. One of these factors is the cell-division-cycle 48 (cdc 48) complex (p97 in mammals), a AAA ATPase that contributes together with two cofactors to extraction of the substrate from the ER membrane prior to proteasome targeting. Following extraction cdc48 might deliver substrates to the proteasome. The 26S proteasome involved in degradation of ubiquitylated substrates consists of two subunits. In the 19S proteasome subunit ubiquitin receptors including regulatory particle non-ATPase-13 (Rpn13), Rpn10 and regulatory particle ATPase-5 have been found with Rpn13 probably mediating the highest affinity binding and playing a pivotal role in degradation. Rpn10 is thought to bind to and then drive substrates into the 20S proteasome core for degradation
In addition, it has been proposed that CDC48- and proteasome-interacting factors might ensure that a polypeptide is not sterically hindered from entering the catalytic chamber of the proteasome. Furthermore, proteasome-associated enzymes and integral proteasome subunits have been shown to mediate substrate de-ubiquitylation which could give substrates a second chance to escape degradation (Nakatsukasa and Brodsky, 2008; Vembar and Brodsky, 2008)

2.6. Unfolded Protein Response:

The accumulation of unfolded proteins can lead to the induction of the unfolded protein response (UPR) in order to reduce protein accumulation in the ER. In yeast the monitor of protein folding is inositol-requiring protein-1 (Ire1), an ER-localized transmembrane Ser/Thr kinase and site-specific endoribonuclease. Under normal conditions, immunoglobulin binding protein (BiP) binds to Ire1 in the ER lumen and maintains the enzyme inactive. When misfolded proteins accumulate in the lumen of the ER BiP binds to the misfolded substrates and therefore Ire1 is activated. Possibly Ire1 might also be activated by dimerization and direct binding to misfolded proteins owing to the formation of a peptide-binding pocket in the ER-luminal domain. Activation of Ire1 results in the transphosphorylation of its cytoplasmic domain which triggers endoribonuclease activity and thus an intron in the mRNA that encodes Hac1p, a UPR transcriptional activator is spliced. The resulting processed mRNA is

re-ligated by tRNA ligase, Rlg1 and translated. Hac1p translocates into the nucleus and binds to UPR elements (UPREs) and possibly other sequences in the promoter region of target genes to upregulate their expression.

In mammals, the UPR involves three transducers, IRE1, PERK and activating transcription factor-6 (ATF6). IRE1 acts identically to its yeast homologue, ER-stress-activated PERK is a transmembrane kinase that phosphorylates the α-subunit of the eukaryotic translation initiation factor-2 (eIF2α), and thus inhibits protein translation. ATF6 traffics to the Golgi under conditions of ER stress where it is proteolytically processed by the S1P and S2P intramembrane proteases to release the ATF6-fragment transcription factor. The resulting fragment translocates into the nucleus where it upregulates target genes. In each case, BiP is also required for transducer activation. It is believed that the IRE1 branch of the UPR seems to be anti-apoptotic, whereas persistent PERK signaling might trigger apoptosis (Vembar and Brodsky, 2008; Lin et al., 2007).
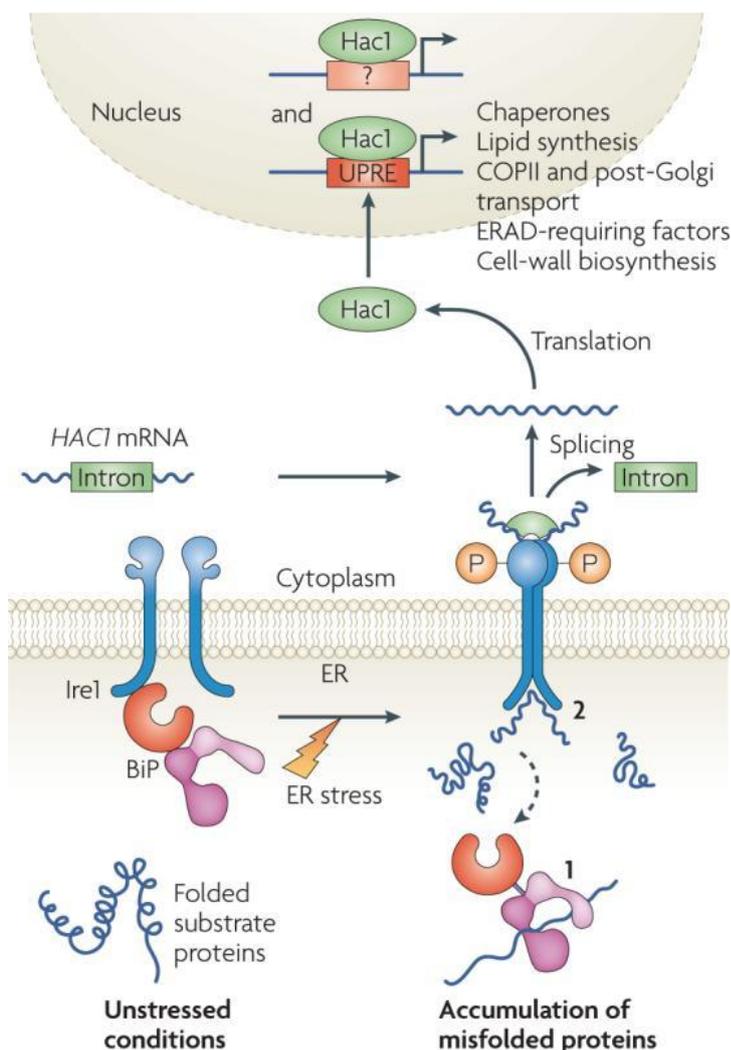
Figure 6 Depiction of the unfolded protein response in yeast (Vembar and Brodsky, 2008)

2.7. Interplay between ERAD and other pathways:

The ERAD pathway is tightly linked to other cellular pathways, although the mechanisms underlying these cross-pathway communications remain to be investigated. The accumulation of misfolded proteins in the ER puts ER and cellular homeostasis at risk (Vembar and Brodsky, 2008). An intimate coordination between ERAD and UPR has been shown in several studies suggesting that an efficient ERAD requires an intact UPR, and UPR induction increases ERAD capacity (Walter et al., 2000; Casagrande et al., 2000; Spear and Walter, 2000; Friedlander et al., 2000). A subset of factors required for ERAD is induced by UPR which is activated by accumulation of misfolded proteins (Kimata et al., 2007; UPR see figure 6). Reduction of stress within the ER is also mediated by other mechanisms such as expansion of the ER volume trough elevated lipid synthesis, augmentation of molecular chaperones and enzymes, decrease of protein translation and translocation into the ER and increase of the secretory pathway (Vembar and Brodsky, 2008). ER-stress-induced autophagy represents another backup mechanism for ERAD in which portions of the ER together with proteins and protein aggregates are engulfed by autophagosomes and further delivered to the lysosome or vacuole for degradation (Nair and Klionsky, 2005). In case that ER stress cannot be overcome, apoptosis can be induced. Several models have been suggested how ER-stress is linked to the apoptotic pathway, however, the ER-stress signal seems to be transmitted by the mitochondria leading to the induction of the the mitochondrial intrinsic apoptotic pathway (Rao et al., 2004).

2.8. The secretory pathway:

Successfully assembled and modified proteins leave the ER and are further transported along the secretory pathway to their final destination. Exit of proteins from the ER occurs at the so-called ER exit sites (ERES), where buds or small membrane clusters contiguous with the ER membrane are formed and coated with the COPII (coat protein complex II) coat resulting in transport vesicles destined for the golgi apparatus (Ellgaard and Helenius, 2003; Barlowe, 2002). Many proteins destined for the secretory pathway exhibit ER export signals which interact with either COPII components or with ER export cargo receptors. However, others do not possess these signals and might depart in a bulk-flow manner (Barlowe, 2003). Although an active mechanism for retaining misfolded proteins in the ER has been proposed, it was shown that a number of misfolded proteins exit the ER and are transported to the Golgi (Kincaid and Cooper, 2007). The forward transport of secretory proteins from the ER is balanced by a retrograde transport performed by COPI-coated vesicles. The COPI coat is molecularly different from the COPII coat and is believed to serve to recycle components needed for ER-vesicle formation and to retrieve escaped ER-resident proteins (Schekman

and Orci, 1996; Barlowe, 2003). Exit from the ER of certain glycoproteins is mediated by specific transporter molecules which concentrate their substrates into forward transport vesicles. One of the best characterized transporter molecules in mammals is ERGIC (Endoplasmic Reticulum-Golgi Intermediate Compartment) -53, a hexameric transmembrane lectin found mainly and in high amounts in the ERGIC (Anelli and Sitia, 2008).

 After leaving the ER, secretory proteins are transported via the ERGIC to the Golgi, where they are further modified to be transported to the extracellular space or the lysosomes. Some of the misfolded proteins are transported to the ERGIC or Golgi before retrotranslocation and degradation. Accumulation of non-native proteins can lead to ER-stress responses such as UPR, autophagy and ERAD (Anelli and Sitia, 2008; see figure 7).
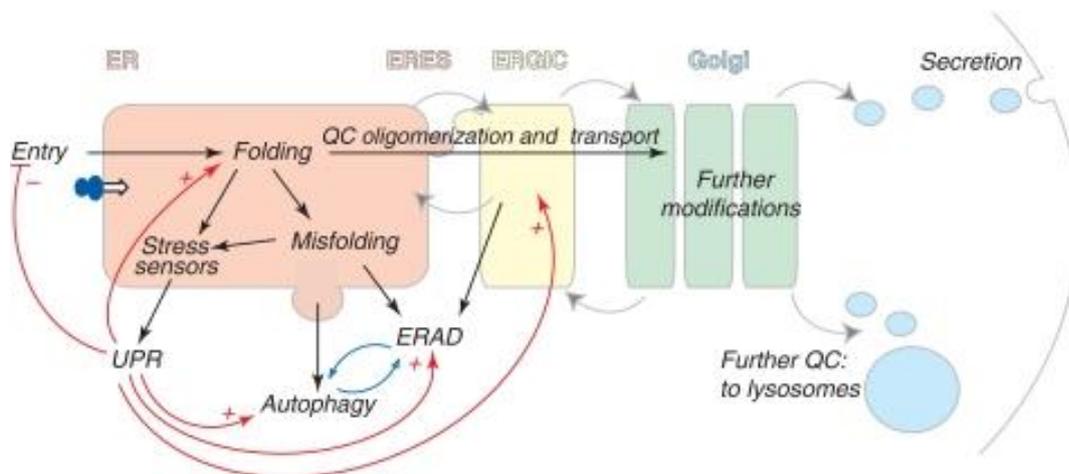
Figure 7 The early secretory pathway. Gray arrows indicate the direction of vesicles moving among different compartments; dark arrows indicate the pathways followed by cargoes in the early secretory pathway; red lines show homeostatic control pathways (+ stimulatory, − inhibitory)(Anelli and Sitia, 2008)

2.9. Diseases:

Defects in protein folding, degradation of misfolded proteins, transport of proteins along the secretory pathway and stress sensing and signaling lead to a multitude of different diseases including cystic fibrosis, antitrypsin deficiency and protein aggregation diseases such as certain forms of Parkinson's, Alzheimer's and prion-associated diseases (Vembar and Brodsky, 2008).

Improvement in understanding of these pathways will increase the possibilities of treatment of many severe chronic diseases (Anelli and Sitia, 2008).

2.10. Introduction to particular topics of this work:

2.10.1. Ribophorin I and variants of Ribophorin I:

The transfer of the oligosaccharide onto asparagines side chains of nascent polypeptides during asparagine-linked glycosylation (ALG) in eukaryotic cells is catalyzed by the oligosaccharyltransferase (OST, see 2.4.1.). One of the subunits of this hetero-oligomeric protein complex is ribophorin I (RI) (Kelleher and Gilmore, 2006), a rough ER transmembrane glycoprotein with the relative molecular mass of 65kDa. After scission of the signal sequence the type I membrane protein RI is 583 amino acids long and consists a cytosolic, a luminal and hydrophobic transmembrane domain. The luminal domain of RI contains at position 275 an asparagine residue representing the N-glycosylation site (Harnik-Ort et al., 1987).

The ERAD substrate and truncated version (relative molecular mass of 38kDa) of RI, RI_{332}, containing only the N-terminal $_{332}$ amino acids of the luminal domain of ribophorin I has been constructed as a model for aberrant proteins being substrates to the ERAD pathway. Furthermore the HA-tagged version, RI_{332}-6HA, has been employed as well. RI_{332}-6HA represents the HA-epitope-tagged variant of RI_{332} with six hemagglutinin tags on the C-terminus. In contrast to the stable full length ribophorin I ($t_{1/2}$ = 25 h), the truncated versions RI_{332} and RI_{332}-6HA are rapidly degraded ($t_{1/2}$ less than 50 min) via the ERAD pathway and have been demonstrated to interact with calnexin (de Virgilio, 1998; Ermonval et al., 2001; Tsao et al., 1992).
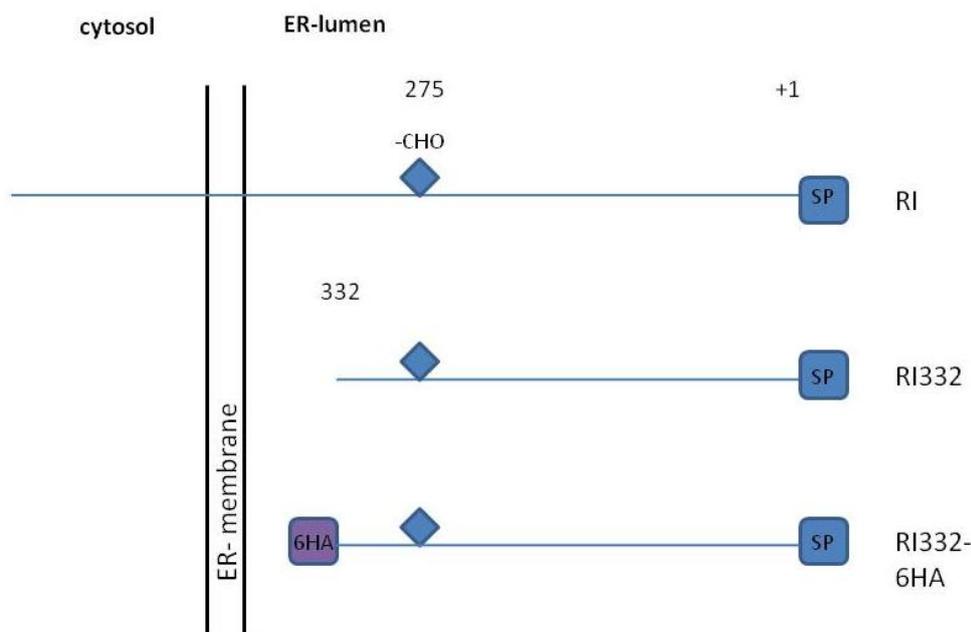
Figure 8 RI variants, SP: signal peptide, -CHO: N-glycosylation site, 6HA: six repeats of the HA epitope

2.10.2. Cell lines used:

The cell lines used for this work were G3 (wild type) and QC (mutant, UDPG:PP-deficient) Chinese hamster lung fibroblasts. G3 cells, also known as Don cells, and QC cells, as well known as DonQ cells have been previously isolated in former studies. QC cells possess a mutation in the UDP-glucose pyrophosphorylase (UDPG:PP) gene leading to low levels of UDP-glucose (Flores-Diaz et al., 1997; 1998, 2004).

Both cell lines were transfected with pZeoSV plasmids containing the cDNAs encoding either the truncated RI332 or its tagged variant RI-332-6HA model protein resulting in 4 different cell lines:

G3 (wild type) cells expressing RI_{332}: $G3RI_{332}$ Cl.4

G3 (wild type) cells expressing RI_{332}-6HA: $G3RI_{332}$-6HA Cl.20

QC (mutant) cells expressing RI_{332}: $QCRI_{332}$ Cl.GG

QC (mutant) cells expressing RI_{332}-6HA: $QCRI_{332}$-6HA Cl.5

Given that QC cells lack glucosylation of the N-glycan of the shortened variants of ribophorin I, RI_{332} and its tagged variant RI_{332}-6HA are expected to possess a GlcNAc2-Man9 N-glycan structure lacking the Glc3 moiety added in wild type cells (G3) (Flores-Diaz et al., 1997; 1998, 2004). Thus, the proteins lacking the glucose-residues might not enter the calnexin/calreticulin cycle and therefore be degraded similar to non-glycosylated proteins, i.e. faster.

2.10.3. Inhibitors:

In this work experiments using inhibitors of proteasomal degradation and N-glycan processing were performed to analyse their influence on processing and degradation of glycoproteins.

The inhibitors used include the proteasome inhibitor ZLLL (carbobenzoxy-L-leucyl-L-leucyl-L-leucinal), as well as dMM (1-deoxymannojirimycin) and kifunensine, the latter two inhibitors of the ER α1, 2- mannosidase I. Furthermore, experiments using castanospermine inhibiting glucosidase I and II were performed.

3. Materials:

3.1. Chemicals and Reagents:

Autoradiography enhancer EN^{3}HANCE	Perkin Elmer
Ethanol 70%	Brenntag
Isobutanol	Merck
Methanol 100%	Fluka
NEC-811 Protein Molecular Weight Marker [Methyl-^{14}C] methylated (973,1 KBq/mg)	Perkin Elmer
NEG-072 EXPRE35S35S [35S]-Protein Labelling Mix (43,5 TBq/mmol)	Perkin Elmer
Neomycin G-418 Sulfate	PAA
Penicillin (10.000 units/ml) and Strepromycin (10.000 units/ml), (Pen/Strep)	Gibco
Protein A Sepharose Beads ^{TM} CL4B	GE Healthcare
Sodium Dodecyl Sulfate (SDS)	AppliChem
Tetramethylethylendiamin (TEMED)	Merck
Trypsin-EDTA 5% (10x)	Gibco
Triton X 100	Amresco
2-Mercaptoethanol for electrophoresis,>98%	Sigma

3.2. Inhibitors:

Inhibitor	Final Concentration	Solvent	Inhibits…	Company
dMM *	2mM	ddH$_2$O	ER α1, 2-mannosidase	TRC
ZLLL*	50µM	DMSO	Proteasome	Peptides
Kifunensine	2µg/ml	ddH$_2$O	ER α1, 2-mannosidase	TRC
Castanospermine	1mM	ddH$_2$O	Glucosidase I and II	TRC

*dMM: deoxy-mannojirimycin; ZLLL: carbobenzoxy-l-leucyl-l-leucyl-l-leucinal

3.3. Equipment:

Cell culture dishes Ø 100 x 20 mm [93100] (10cm dishes)	TPP
Cell culture test plate 6 [92006] (6 well plate)	TPP
Cell Incubator	Binder
Centrifuge 5415C	Eppendorf
Cooling Centrifuge 1K15	Sigma
Film Cassette	Sigma
Film Developer Curix60	AGFA
Flow Hood Laminair HB 2448	Holten
Gel Dryer SGD 4050	Savant
Gel Electrophoresis Power Supply	Biorad
Gel Electrophoresis Apparatus	Biorad
Heating Block Thermomixer 5436	Eppendorf
Inverted Microscope ID03 Binocular	Zeiss
Vacuum Pump DIVAC 2,4L	Leybold
Waterbath TWB 14	Julabo
Whatman Paper	Whatman
X-ray Film Omat Blue XB-1	Kodak

3.4. Buffers and Solutions:

<u>Fixing Solution</u>

5% (v/v) Methanol	Merck
15% (v/v) Acetic Acid	Merck

<u>PBS (pH 7,4)</u>

27,4mM NaCl	Sigma Aldrich
54µM KCl	AppliChem
2mM Na_2HPO_4	Merck
340µM KH_2PO_4	Merck

Reducing Sample Buffer

Sample Buffer:

50mM Tris	Amresco
0,1% Bromophenol Blue	AppliChem
2% SDS	Amresco
10% Glycerol	Sigma
+ 3% β -Mercaptoethanol	Sigma

Running Buffer (10x)

25mM Tris	Amresco
192mM Glycine	AppliChem
1% SDS	Amresco

SDS Lysis Buffer (pH 7,4)

95mM NaCl	Sigma Aldrich
25mM Tris/HCl	Amresco
3mM EDTA	Amresco
1% SDS	AppliChem
4% Complete Protease Inhibitor Stock (25x)	Roche

SDS Wash Buffer (pH 7,4)

95mM NaCl	Sigma Aldrich
25mM Tris/HCl	Amresco
3mM EDTA	Amresco
1, 25% Triton X 100	Amresco
0, 2% SDS	AppliChem
1% Complete Protease Inhibitor Stock (25x)	Roche

Solution I for Polyacrylamide Gels

30%(w/v) Acrylamide	USB
0,6%(w/v) Bis-Acrylamide	USB

Solution IIA for Polyacrylamide Gels

3M TrisHCl pH 8,9   Merck

Solution IIB for Polyacrylamide Gels

1M TrisHCl pH 6,7   Merck

10% SDS- Polyacrylamide Gels- Separation Gel

3,33ml Solution I   USB
1,26ml Solution IIA   Merck
5,34ml dH2O
54µl 20% SDS   Amresco
5µl TEMED   Merck
50µl 10% APS   Biorad

10% SDS- Polyacrylamide Gels - Stacking Gel

0,75ml Solution I   USB
0,63ml Solution IIB   Merck
3,6ml dH2O
25µl 20% SDS   Amresco
5µl TEMED   Merck
25µl 10% APS   Biorad

3.5. Cell Culture Media:

Growth Medium

RPMI – 1640   Gibco
-L-Glutamine
+D-Glucose
+ 1% L-Glutamine   Gibco
+ 1% Pen/Strep   Gibco
+ 10% Fetal Calf Serum (FCS)   Gibco
400µg/ml G-418 Sulfate   PAA
400µg/ml Zeocine   Invitrogen

Trypsin-EDTA Solution

PBS (pH 7,4)
+ 10% Trypsin-EDTA (10x)   Gibco

Freezing medium

10% DMSO   Sigma
90% FCS   Gibco

Starvation Medium

RPMI – 1640   Gibco
- L-Glutamine
- L-methionine
- L-Cysteine
- L-Cystine
+ 1% L-Glutamine   Gibco

Pulse Medium

Starvation Media   Gibco
+ 2,5% L- [35S] Methionine (11mCi/ml)   Perkin Elmer

Chase Medium

Growth Media   Gibco
+ 5mM Methionine (unlabeled)

3.6. Cell lines:

The cell models used in this study were G3 cells representing the wild type, and QC cells
representing the mutant cell line. The pre-existing cell model, DonQ cells, was obtained
through mutagenesis with ethyl methanesulfonate and selection for resistance to Clostridium
difficile toxins A and B (Florin, 1991). Since they are UDPG:PP (uridine diphosphate
glucose:pyrophosphorylase) – deficient, they persistently display low levels of UDP-glucose

as well as UDP-galactose. DonQ cells were stably transfected with a plasmid carrying the cDNA of the human wild type UDPG-PP gene. This resulted in the generation of G3 cells, revertants of the mutant DonQ cell line depicting the wild type phenotype. Stable transfection of DonQ cells with an empty vector generated the QC cell line, displaying the UDPG-PP-deficient, mutant phenotype (Florin, 1991; Flores-Díaz et al., 1997). Both, G3 and QC cells, were obtained from Dr. Stuart Moore (INSERM, U773, Paris, France).

Both cell lines were transfected with pZeoSV plasmids carrying either the cDNA of the model protein RI_{332} or its tagged version RI_{332}-6HA. Afterwards, cell clones were isolated and tested for expression of RI_{332} or RI_{332}-6HA. Only cells expressing the constructs were cultivated further and stored in liquid nitrogen tanks.

Cell line	Transfected with	Clone name
G3 (wild type)	RI_{332}	G3 RI_{332} Cl. 4
G3 (wild type)	RI_{332}-6HA	G3 RI_{332} 6HA Cl. 20
QC (UDPG:PP-deficient)	RI_{332}	QC RI_{332} Cl. GG
QC (UDPG:PP-deficient)	RI_{332}-6HA	QC RI_{332} 6HA Cl. 5

3.7. Antibody:

Anti-RI-lum polyclonal antibody:

Recognizes the luminal domain of Ribophorin I

Abbreviation: α-RI-lum and α-RI

Host animal: rabbit

Immunoprecipitation: 2µl/ IP

Reference: de Virgilio et al., 1998; 1999; Ermonval et al., 2001; Kitzmueller et al., 2003

4. Methods:

4.1. Cell Culture:

4.1.1. Seeding of cells:

Cryogenic tubes, each one containing one of the four cells lines used in this work, were taken from liquid nitrogen storage tanks and cells were thawed quickly in a 37°C waterbath. Subsequently, the cells were added to 10ml growth medium (37°C) in a falcon tube. To remove the cryoprotectant DMSO, the cells were then centrifuged at 1300rpm for seven minutes. After taking off the supernatant the cell pellet was suspended in 15ml growth medium and added to 10cm dishes. The dishes were placed into cell incubators and stored at 37°C and 5% CO_2. The following day, growth medium was aspirated and replaced by 10ml new growth medium.

4.1.2. Cultivation of cells:

For growth, the cells were incubated at 37°C and 5% CO_2. Their density and condition were controlled by light microscopy. Confluent 10cm dishes corresponded to about 10 million cells. If about 80% density was reached, cells were split into new 10cm dishes. Therefore, the growth medium was taken off and cells were rinsed with 10ml PBS (37°C) to remove dead cells and cell debris. Thereafter, 1,5ml trypsin-EDTA-solution was added, and cells were incubated for two to five minutes in the cell incubator in order to detach the cells from the dishes. To stop the tryptic digest 8ml of growth medium was added to the dishes. Gentle pipetting resulted in a homogenous suspension of cells that was split onto new 10cm dishes. Additional growth medium was added to reach a total volume of 10ml. The volume of the cell suspension added to the new dishes was dependent on the required split ratio. Cells were incubated as mentioned above. In case cells had not to be split, medium was changed at least every three days.

4.1.3. Storage of cells:

As a first step to freeze cells, growth media were removed and dishes were rinsed twice with 5ml PBS at 37°C. Subsequently, 1,5ml trypsin-EDTA solution was added and cells were incubated for two to five minutes. Then, growth medium was added to stop the tryptic digest. The resulting cell suspension was added to falcon tubes and centrifuged at 1300rpm for seven minutes. Afterwards, the supernatant was taken off and the pellet was resuspended in ice-cold freezing medium containing 10% DMSO. The suspension was added to cryotubes and frozen at -80°C (-1°C/minute). For long-time storage cells were kept in liquid nitrogen.

4.2. Pulse-Chase Experiments:

4.2.1. Splitting of cells onto 6-well plates:

In preparation for radioactive labeling experiments cells were split onto 6-well plates and incubated at 37°C and 5% CO_2 over night. Each 6-well plate used corresponded to timepoint during the chase phase of the experiment. Usually, each pulse-chase experiment was performed for two clones at once, cultivating both clones in two wells, one for the experiment with an inhibitor, one as a control without inhibitor. The next day the cell density was controlled by light microscopy. If confluence reached between 70% and 90% the experiment was performed.

4.2.2. Pre-incubation of cells:

In case of application of inhibitors, cells were pre-incubated at 37°C, 5%CO_2 in 1ml growth medium containing the inhibitor in the required concentration for 1.5 hours. Control cells were incubated using 1ml growth medium without inhibitor for the same time.

4.2.3. Starvation of cells:

Prior to addition of the starvation medium, cells were rinsed twice with 1ml PBS/ well. Then 1ml of starvation medium with or without inhibitor (control) was added to each well and cells were incubated at 37°C and 5% CO_2 for 30 minutes.

4.2.4. Pulse Phase:

In order to label cells radioactively, starvation medium was aspirated and 700µl pulse medium with or without inhibitor was added to the 6-well plates and incubated for 15 minutes. From this moment on all the following steps were performed in rooms and with equipment designed for radioactive experiments.

4.2.5. Chase Phase:

Following removal of pulse medium, 1ml per well of chase medium was added and cells were incubated for different periods of time, ranging from five to 135 minutes of incubation. For experiments determining degradation times of RI, RI_{332} and RI_{332}-6HA, chase phases were between 5 and 120 minutes long. For experiments with inhibitors chase phases lasted five, 45, 90 and 135 minutes. After each timepoint, 6-well plates were kept on ice, chase medium was taken off and cells were rinsed with 1ml of PBS. From now on, all steps were performed on ice.

4.3. Protein Extraction:

For extraction of proteins, 150µl of SDS lysis buffer pH7,4 were added and cells were scraped from 6-well plates and collected in 1,5ml eppendorf tubes kept on ice. Subsequently, another 150µl of SDS lysis buffer pH 7,4 was added and the procedure was repeated in order to collect as much cell lysate as possible.

After this step had been repeated for each timepoint, the cell lysates were sonicated for ten seconds, put on a heating block and incubated at 95°C for two minutes. Thereafter, 1ml of ice-cold SDS wash buffer pH7,4 was added and the cell lysate was centrifuged at 4°C and 13.000rpm for 15 minutes to remove cell debris.

4.4. Immunoprecipitation (IP):

Following centrifugation, the supernatant was recovered and transferred to a new 1,5ml eppendorf tube on ice. 40µl of protein A sepharose beads (preparation see 4.4.1.) and 20µl of anti-RI-Ium antibody dilution (preparation see 4.4.2.) were added and the lysate was immunoprecipitated by turntabling in the cold room at 4°C over night.

4.4.1. Preparation of protein A sepharose beads:

70mg of protein A sepharose beads were swollen in 1,5ml eppendorf tubes with 1ml of SDS wash buffer at 4°C on the turntable for 30 minutes. Then, the beads were washed three times. Therefore the beads were centrifuged at 8.000rpm for three minutes. The supernatant was removed and the beads were turntabled with 1ml SDS wash buffer for 10 minutes. Finally, the beads were resuspended in 700µl of SDS wash buffer leading to a concentration of 100mg beads/ml.

4.4.2. Preparation of anti-RI-Ium antibody:

A 1/10 dilution of the anti-RI-Ium antibody was achieved by adding 315µl SDS wash buffer to 35µl of anti-RI-Ium antibody.

4.5. Washing of IP:

The following day, the IPs were washed three times with SDS wash buffer. Therefore, the eppendorf tubes containing the IPs were centrifuged at 8.000rpm for three minutes, supernatant was discarded and 1ml of SDS wash buffer was added. Then, the IPs were

turntabled at 4°C for 10 minutes. After washing with SDS wash buffer was completed, the IPs were washed twice with PBS in the same manner.

4.6. SDS- Polyacrylamide Gel Electrophoresis:

4.6.1. Preparation of 10% SDS PAGE Gels:

First, the compounds of the separation gel were mixed, then poured into the gel caster and overlaid with isobutanol. Following polymerization, the stacking gel was mixed and added on top of the separation gel after isobutanol had been completely removed. Then the combs were placed to create the wells and the stacking gel was left to polymerize. Subsequently, the combs could be removed and the gel was placed into the gel apparatus. 1x running buffer was filled into the buffer chambers and thus the gel was ready to be loaded.

4.6.2. Preparation of samples for SDS-PAGE:

After all the washing steps of the IP had been performed, 20µl of sample buffer were added to the beads and the IPs were incubated at 95°C for five minutes in order to dissolve the preticipated proteins from the beads. Then the samples were spun down and the supernatant (20µl) was loaded on 10% SDS-PAGE gels. 5µl of the ^{14}C-marker (1/1 dilution with sample buffer) were loaded on one of the side lanes of each gel.

4.6.3. SDS-PAGE:

The SDS-PAGE was performed at 180V for about 45 minutes. Then, the gels were fixed in fixing solution, enhanced in autoradiography enhancer EN^{3}HANCE and washed in water, each step lasting 30 minutes. The gels were then put on whatman paper soaked in water and dried at 80°C in the gel dryer for 30 to 45 minutes.

4.7. Fluorography:

In the dark room, the dried gels were attached to the film cassette and an X-ray film was placed onto the top. The cassettes were closed and stored at -80°C for several days to two weeks before film development. For development the film cassettes were thawed for about 1 hour at room temperature before they were opened in the dark room to develop the films using the film developer.

4.8. Analysis of the films:

Following the development of the films, band intensities were analyzed to determine the half lives of RI_{332} or RI_{332}-6HA using the software ImageJ (http://rsbweb.nih.gov/ij/), an image processing program. Films were scanned, background was corrected, and the bands corresponding to RI_{332} or RI_{332}-6HA in the different lanes were compared in proportion to each other as well as to endogenous ribophorin I, which is a long-lived protein with $t_{1/2} > 24\,h$, used as a loading control. The relative strengths of the bands representing RI_{332} or RI_{332}-6HA were determined by calculation as follows. The band of RI_{332} (or RI_{332}-6HA) in the lane corresponding to 5 minutes of chase was set to be 100 per cent and the band strengths corresponding to the other chase times were calculated in per cent relative to this band. The values obtained were corrected for the intensities of the bands representing the endogenous ribophorin I in the same lanes, respectively. The results were depicted in percental values in charts. Assuming that RI_{332} or RI_{332}-6HA decrease is following a function of first order, the natural logarithm of the percental values of RI_{332} or RI_{332}-6HA was calculated and depicted in charts, with the x-axis displaying the time and the y-axis displaying the logarithmic values. A best-fit linear line was drawn, and its slope was used to determine the half lives of RI_{332} or RI_{332}-6HA applying the formula $t_{1/2}= \ln(2)/slope$. All calculations and depictions were done using Microsoft Excel software. In cases where degradation intermediates of RI_{332} occur, such as in the presence of ZLLL (see 5.2.1.), these intermediates were included in the determination of RI_{332} band intensities.

5. Results:

5.1. Determination of the degradation kinetics of the model substrates RI_{332} and RI_{332}-6HA in wild type and UDPG:PP-deficient cells:

In order to determine the stability of RI_{332} and RI_{332}-6HA, models for aberrant proteins being substrates to the calnexin/calreticulin cycle and further the ERAD pathway, pulse-chase experiments were performed in wild type (G3) and mutant (QC) cell lines using ^{35}S-labeled methionine, followed by protein extraction and immunoprecipitation with an α-RI-lum antibody, SDS-PAGE, fluorography and computational analysis. Both cell lines are Chinese hamster lung fibroblasts. While G3 cells represented the wild type cell model in this study, QC cells were used as the mutant cell model since they are glycosylation-deficient. Both cell lines stably express the model proteins RI_{332} or RI_{332}-6HA.

Since the endogenous ribophorin I was shown to remain stable ($t_{1/2}$=25h) in preceding experiments (de Virgilio, 1998; Ermonval et al., 2001; Tsao et al., 1992) as well as in the experiments performed in this study, it was used as a loading control to calculate the percental degradation of the model substrates and their half lives.

5.1.1. Degradation kinetics of RI_{332} in wild type and mutant cells:

To compare the degradation of the model substrate RI_{332} in G3 and QC cells, radioactive labeling experiments were performed with a pulse phase of 15 minutes and chase phases of 5, 15, 30, 45, 60, 75, 90 and 120 minutes.

<u>G3-RI_{332} Cl.4:</u>
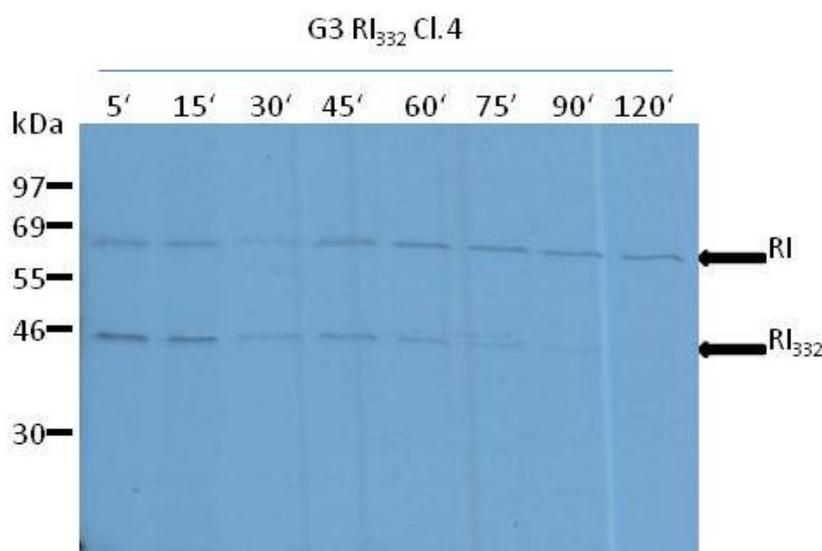
Figure 9 Fluorography of G3-RI_{332} Cl.4
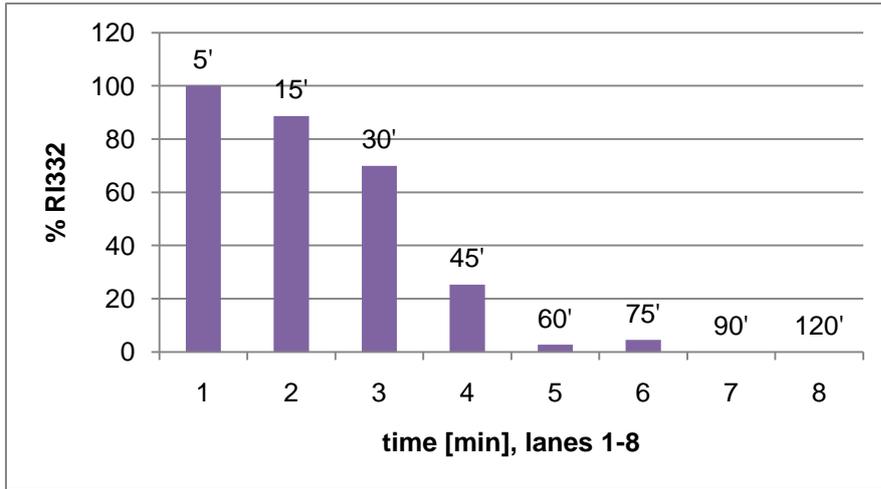
Figure 10 Degradation of RI_{332} in G3 cells, %RI_{332} during 5 to 120 minutes

While the endogenous ribophorin I remains stable throughout all timepoints and is detected as a band with an apparent mass of 65kDa, RI_{332}, which is seen as a band at about 45kDa, is rapidly degraded (see figure 9). The degradation of RI_{332} is depicted in percentage values in figure 10 (for the calculation see 4.8.). The half life of the substrate was determined to be 13 minutes (see figure 13).

QC-RI_{332} Cl.GG:
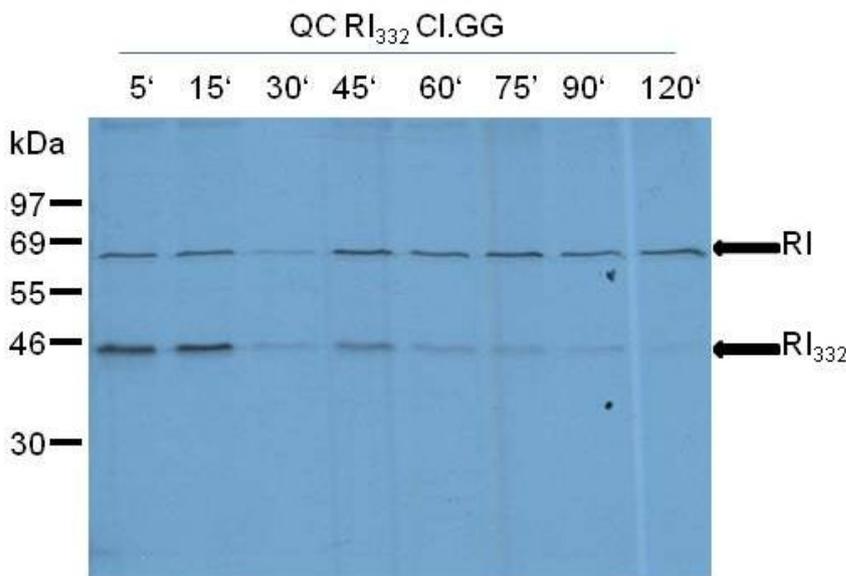
Figure 11 Fluorography of QC-RI_{332} Cl.GG
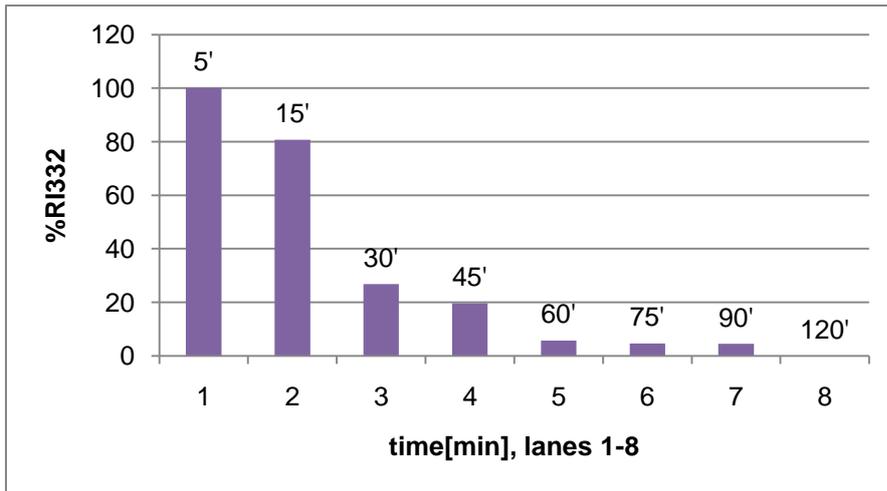
Figure 12 Degradation of RI_{332} in QC cells, %RI_{332} during 5 to 120 minutes

Concerning QC cells, for endogenous ribophorin I a band can be detected at about 65kDa that remains stable during the chase. RI_{332}, corresponding to the lower band in figure 11, is rapidly degraded. In figure 12, percental degradation of the model protein is illustrated. The determined half life is 17 minutes, that means slightly higher than in wild type cells (see figure 13).
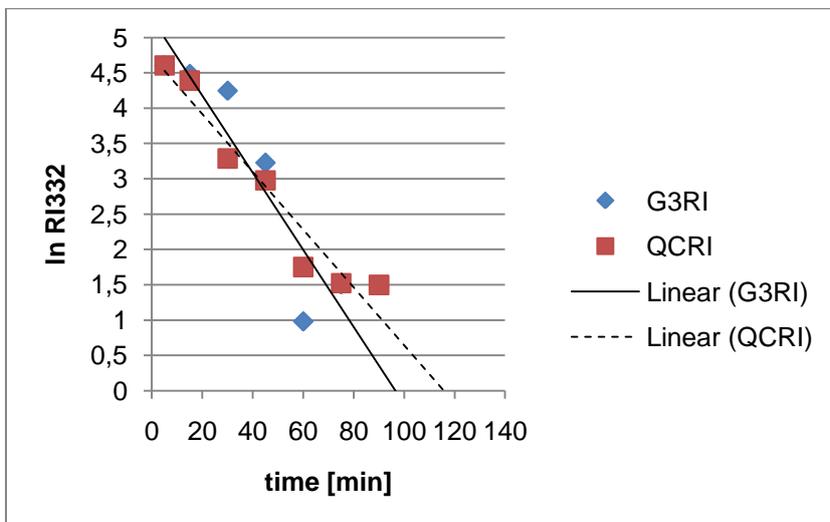
Figure 13 Determination of the half life of RI_{332} in both G3 (wild type, squares, constant line) and QC cells (mutant, rhombs, dashed line)

The half lives of RI_{332} were determined to be 13 minutes for G3 and 17 minutes for QC cells, thus the mutant showed slightly slower degradation of the substrate protein.

This is consistent with the results obtained from a further degradation assay including the same cell lines. The half live was determined to be 22 minutes for G3 cells and 25 minutes for QC cells (data not shown).

5.1.2. Degradation kinetics of RI$_{332}$-6HA in wild type and mutant cells:

For the model substrate RI$_{332}$-6HA radioactive labeling experiments were done as well in wild type and mutant cell lines to gain insight into the degradation differences of aberrant proteins in these cells. Again, the pulse phase lasted for 15 minutes, chase phases were 5, 15, 30, 45, 60, 75, 90, and 120 minutes.

G3-RI$_{332}$-6HA Cl.20:
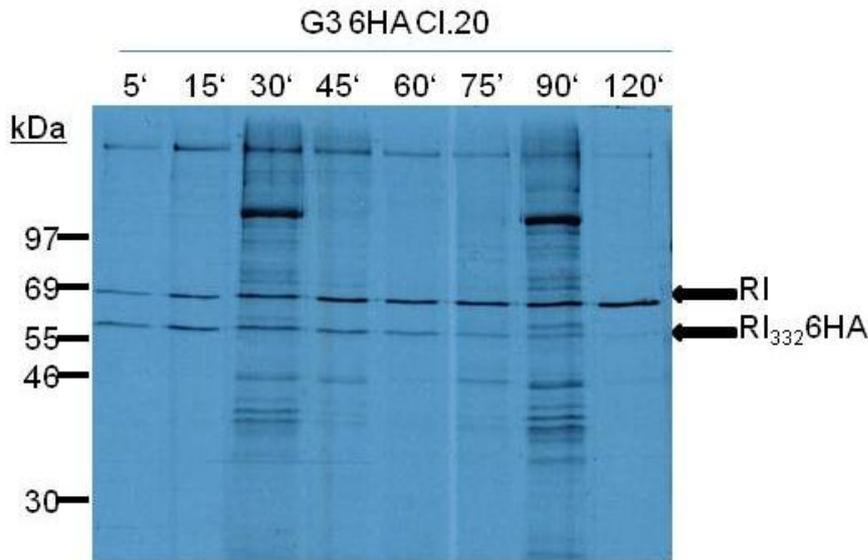
Figure 14 Fluorography of G3-RI$_{332}$-6HA Cl.20
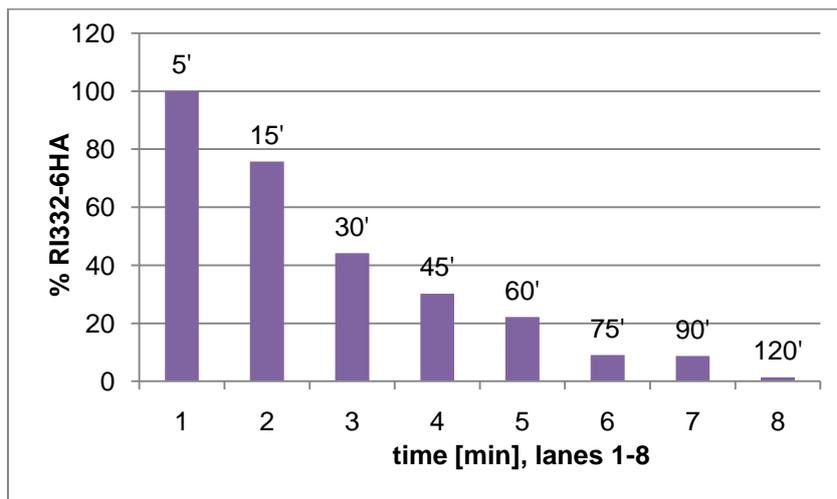
Figure 15 Degradation in G3 cells, %RI$_{332}$-6HA during 5 to 120 minutes

Once more, the endogenous ribophorin I can be detected at 65kDa as a stable band throughout all timepoints. However, RI$_{332}$-6HA, detected at about 55kDa, is degraded (see

figure 14). Figure 15 shows the degradation of RI_{332}-6HA in percentage values. The half life of RI_{332}-6HA was calculated to be 20 minutes (see figure 17).

QC-RI_{332}-6HA Cl.5:
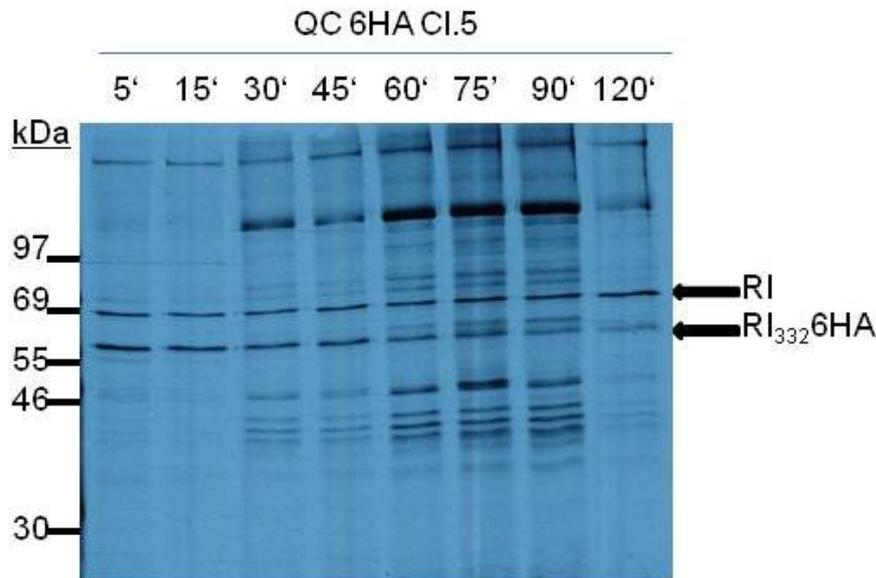
Figure 16 Fluorography of QC-RI_{332}-6HA Cl.5
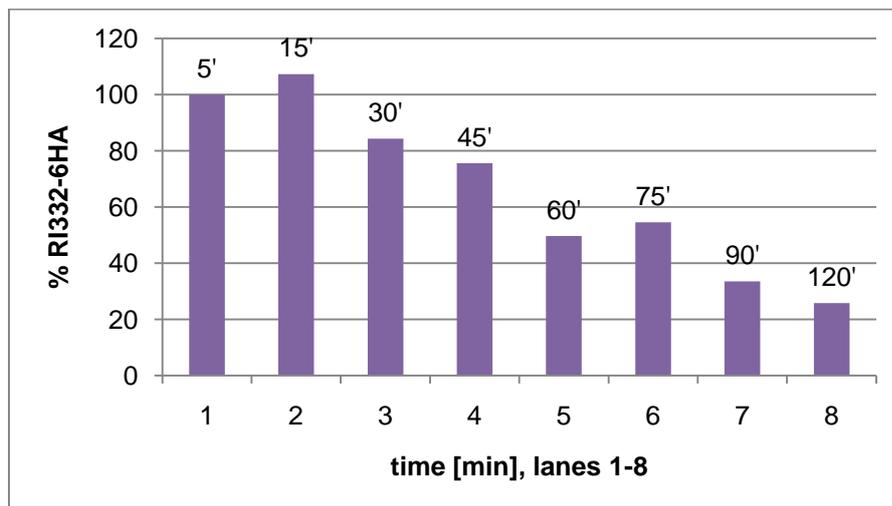
Figure 16 Degradation in QC cells, %RI_{332}-6HA during 5 to 120 minutes ($t_{1/2}$= 51min)

In UDPG:PP-deficient QC cells, RI_{332}-6HA shows rapid degradation as well. However, degradation appears to be slower in mutant than in wild type cells with a half life for RI_{332}-6HA of 54 minutes (see figure 17).
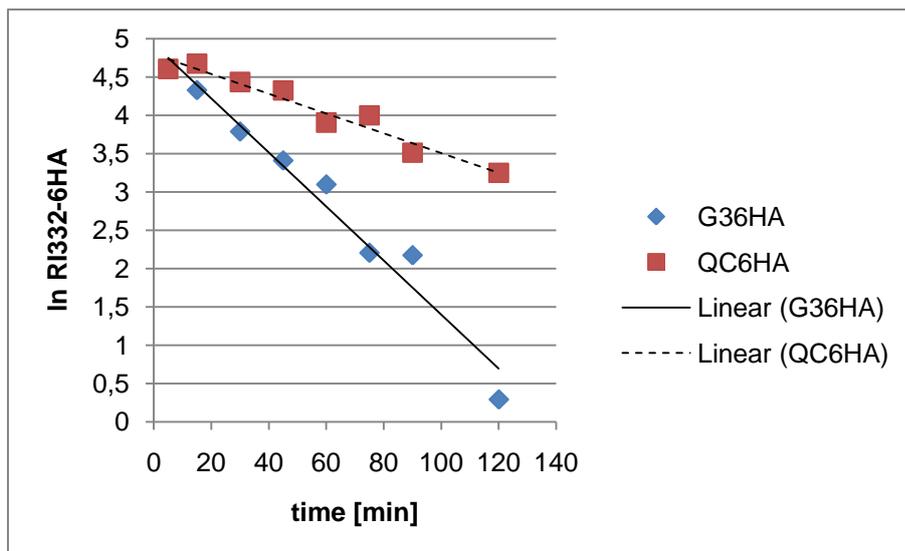
Figure 17 Determination of the half life times for RI_{332}-6HA in both G3 (wild type, squares, constant line) and QC cells (mutant, rhombs, dashed line)

Degradation of RI_{332}-6HA was found to be faster in G3 cells with a half life of 20 minutes compared to QC cells, where the half life was determined to be 54 minutes.

This is consistent with the results obtained from another degradation assay including the same cell lines with calculated half lives of 35 minutes for G3 cells and 64 minutes for QC cells (data not shown).

Calculation of the mean value and standard deviation:

In order to calculate the mean values of the half lives concerning the kinetics of all four clones, half life values gained from the experiments determining the degradation kinetics as well as the half live values of the controls in the experiments performed with inhibitors (see 5.2.) were used. For QC-RI_{332}-6HA Cl.5 the values calculated in the experiment with dMM was not included.

	G3-RI_{332} Cl.4	**QC-RI_{332} Cl.GG**	**G3-RI_{332}-6HA Cl.20**	**QC-RI_{332}-6HA Cl.5**
t1/2 (mean value ± standard deviation)	24 ± 7min (n=5)	31 ± 15min (n=5)	28 ± 6min (n=6)	58 ± 13min (n=5)

5.2. Analysis of the influence of inhibitors on glycoprotein processing and degradation:

Based on observations in preceding studies with HeLa cells (Kitzmueller et al., 2003) experiments using inhibitors of proteasomal degradation such as ZLLL and inhibitors of N-glycan processing such as castanospermine, dMM and kifunensine were performed to gain insight into their influence on glycoprotein processing and degradation in the ER.

For that purpose, pulse-chase experiments were done with either ZLLL, castanospermine, dMM or kifunensine. First, cells were pre-incubated for 90 minutes with the inhibitor in growth medium. Then, the experiment was carried out in the same way as the degradation kinetics experiments with all media used containing the inhibitor. As a control, the experiments were done without inhibitors in parallel.

5.2.1. Analysis of the influence of ZLLL:

To study the influence of the proteasomal inhibitor ZLLL on the degradation of the model substrates RI_{332} and RI_{332}-6HA, 50µM ZLLL were applied and pulse-chase experiments were performed.

G3-RI_{332} Cl.4:
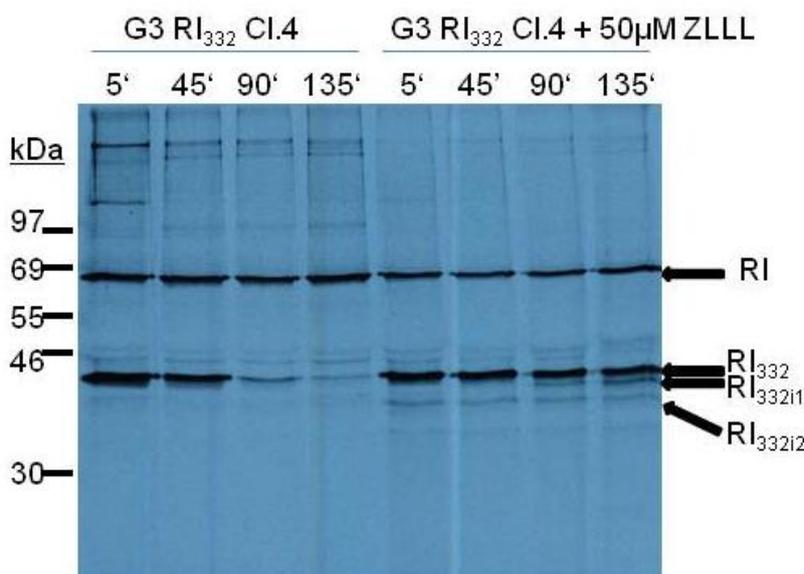
Figure 18 Fluorography of G3-RI_{332} Cl. 4 ± 50µM ZLLL
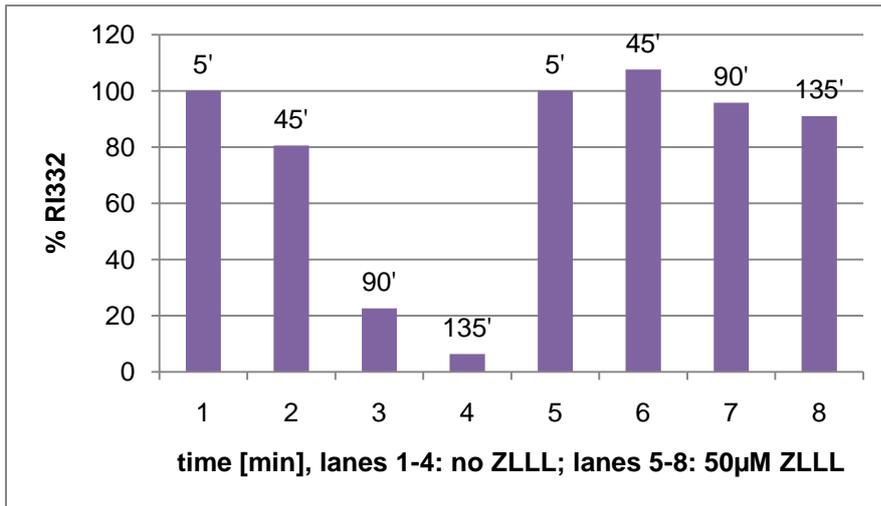
Figure 19 Degradation of RI$_{332}$ in G3 cells, %RI$_{332}$ during 5 to 135 minutes ±ZLLL
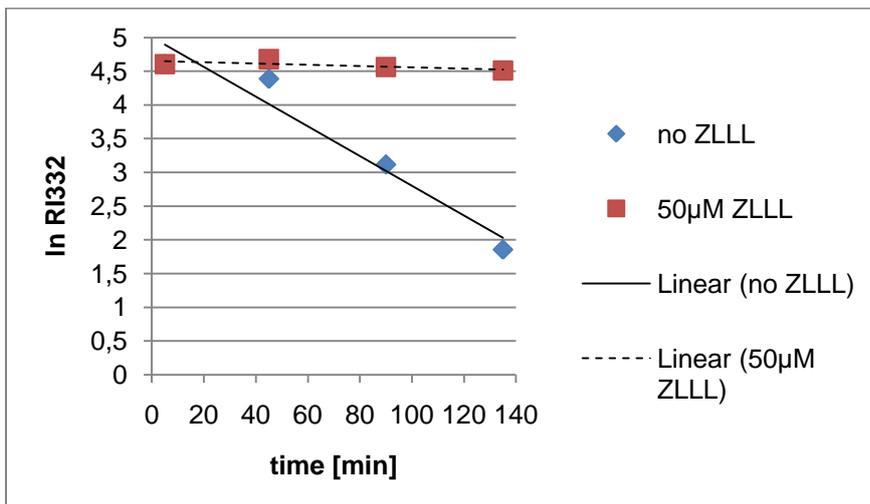
Figure 20 Determination of the half life of RI$_{332}$ in G3 cells (no ZLLL: squares, constant line; 50µM ZLLL: rhombs, dashed line)

No ZLLL: t$_{1/2}$= 31min

50µM ZLLL: t$_{1/2}$= 770min

In wild type cells, application of the proteasomal inhibitor ZLLL strongly affects the stability of the model substrate RI$_{332}$. The calculated half life rose from 31 minutes without ZLLL to 770 minutes with ZLLL. In addition to the band representing RI$_{332}$ at about 45kDa, two additional bands (RI$_{332}$i1 and RI$_{332}$i2) slightly lower than the first one could be detected as well. This is consistent with the results of former studies in HeLa cells (Kitzmueller et al., 2003), where the two bands depict degradation intermediates of RI$_{332}$, one glycosylated (RI$_{332}$i1), one un-

glycosylated ($RI_{332}i2$) (see figure 18).The half life of RI_{332} in G3 cells was calculated to be 31 minutes without and 770 minutes with ZLLL (see figure 20).

QC-RI_{332} Cl.GG:
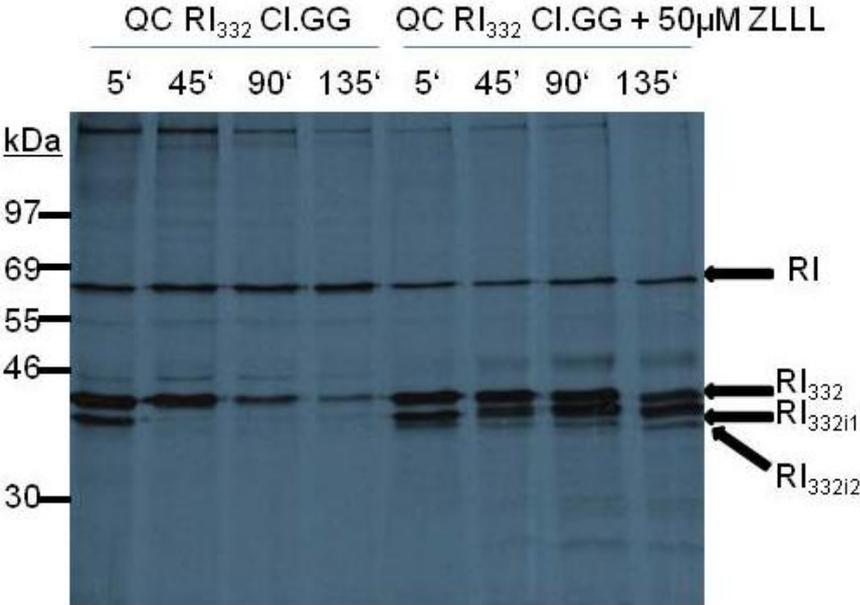
Figure 21 Fluorography of QC-RI_{332} Cl. GG ± 50µM ZLLL
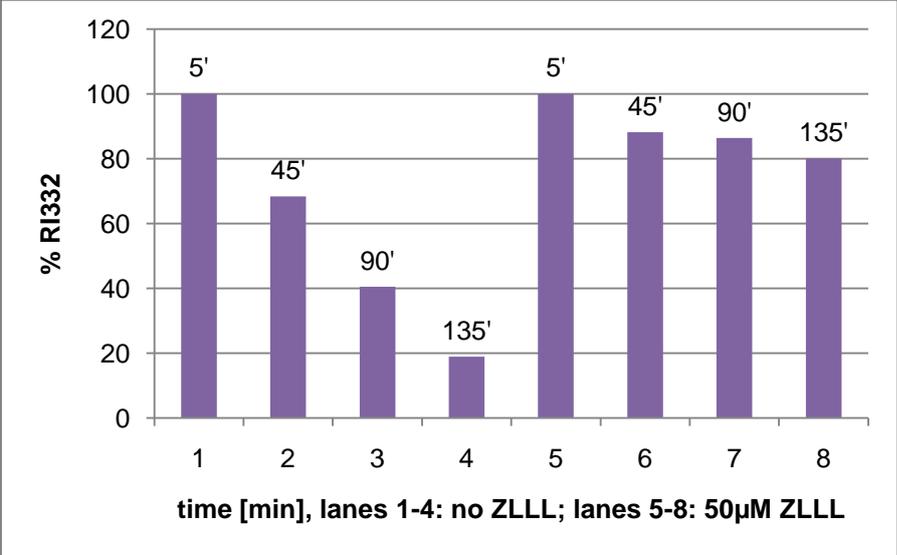
Figure 22 Degradation of RI_{332} in QC cells, %RI_{332} during 5 to 135 minutes ± ZLLL
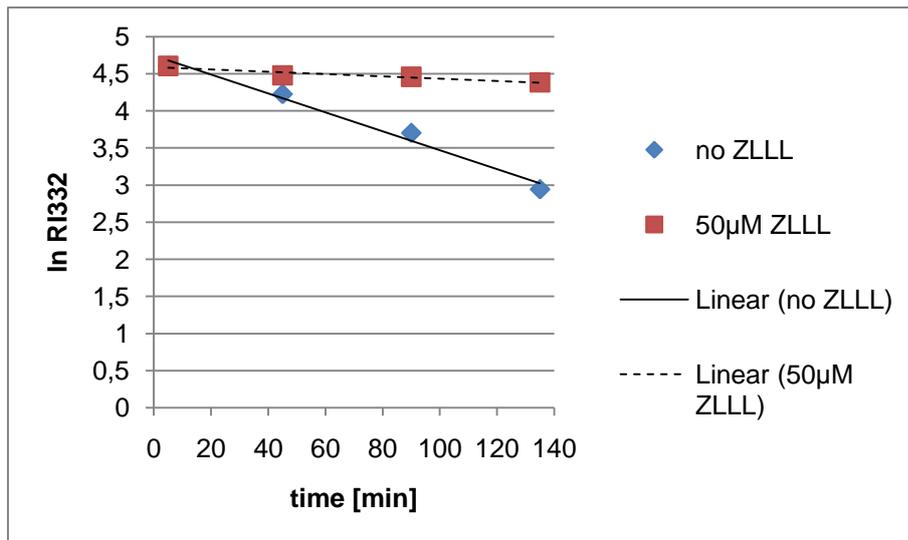
Figure 23 Determination of the half life of RI_{332} in QC cells (no ZLLL: squares, constant line; 50µM ZLLL: rhombs, dashed line)

No ZLLL: $t_{1/2}$= 55min

50µM ZLLL: $t_{1/2}$= 433min

Concerning the QC cells, addition of ZLLL again resulted in stabilization of the model substrate as well as generation of two degradation intermediates, $RI_{332}i1$ and $RI_{332}i2$ (see figure 21). The impact of ZLLL on the mutant cell line was detected as a shift of the half life from 55 minutes without ZLLL to 433 minutes with ZLLL (see figure 23).

ZLLL strongly inhibits RI_{332} degradation in both cell lines exhibiting a stronger effect on G3 cells.
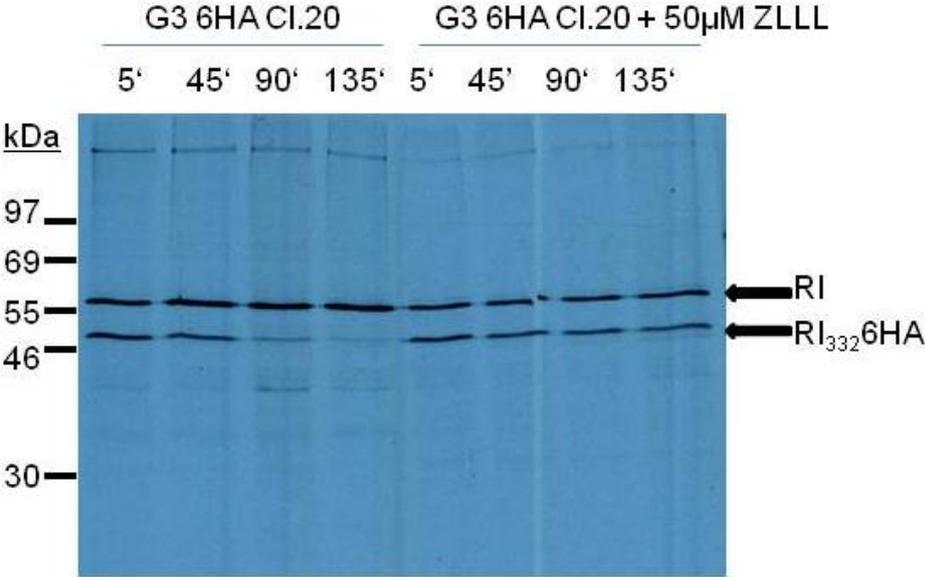
Figure 24 Fluorography of G3-RI$_{332}$-6HA Cl. 20 ± 50µM ZLLL
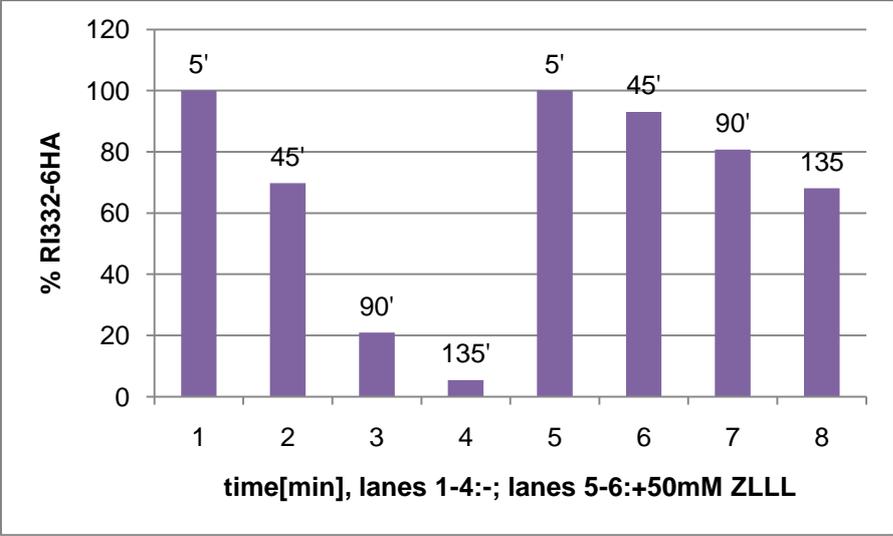
Figure 25 Degradation in G3 cells, %RI$_{332}$-6HA during 5 to 135 minutes ± ZLLL
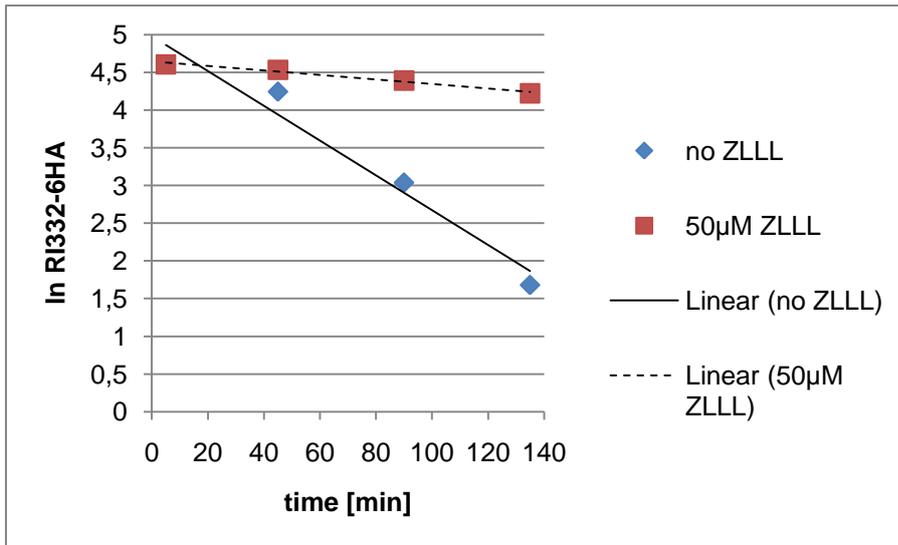
Figure 26 Determination of the half life of RI$_{332}$-6HA in G3 cells (no ZLLL: squares, constant line; 50µM ZLLL: rhombs, dashed line)

No ZLLL: t$_{1/2}$= 30min

50µM ZLLL: t$_{1/2}$= 231min

For wild type cells expressing RI$_{332}$-6HA, ZLLL stabilizes the construct as well, shifting the half life of the model protein from 30 minutes to 231 minutes (see figures 24-26). RI$_{332}$-6HA can be seen at about 55kDa, the expected degradation intermediates are difficult to detect, although one light band appears to be slightly lower to the RI$_{332}$ band (see figure 24).

QC- RI$_{332}$-6HA Cl.5:
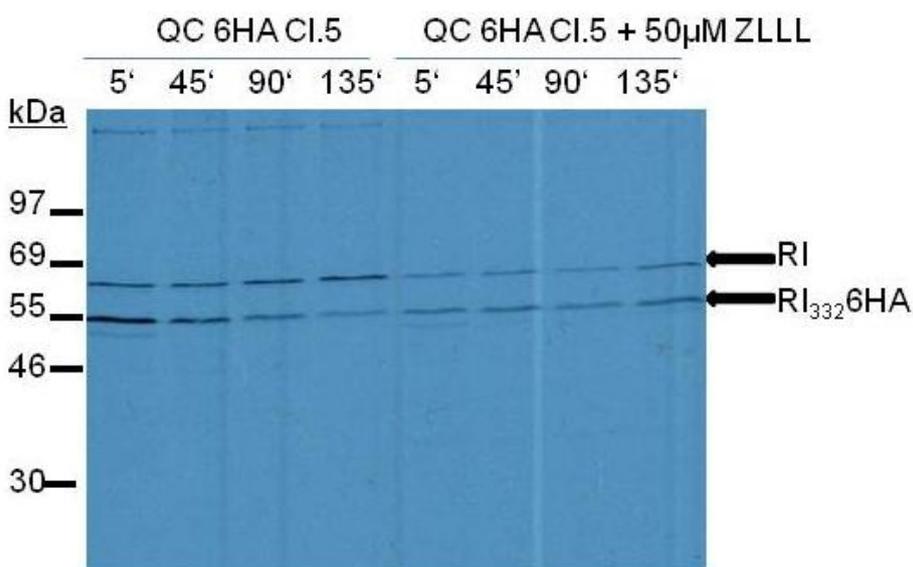
Figure 27 Fluorography of QC-RI$_{332}$-6HA Cl. 5 ± 50µM ZLLL
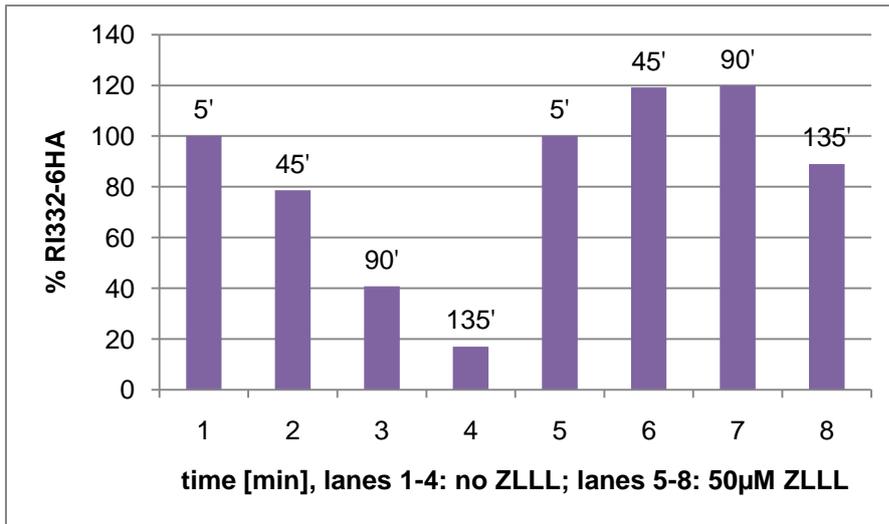
Figure 28 Degradation in QC cells, %RI$_{332}$-6HA during 5 to 135 minutes ± ZLLL
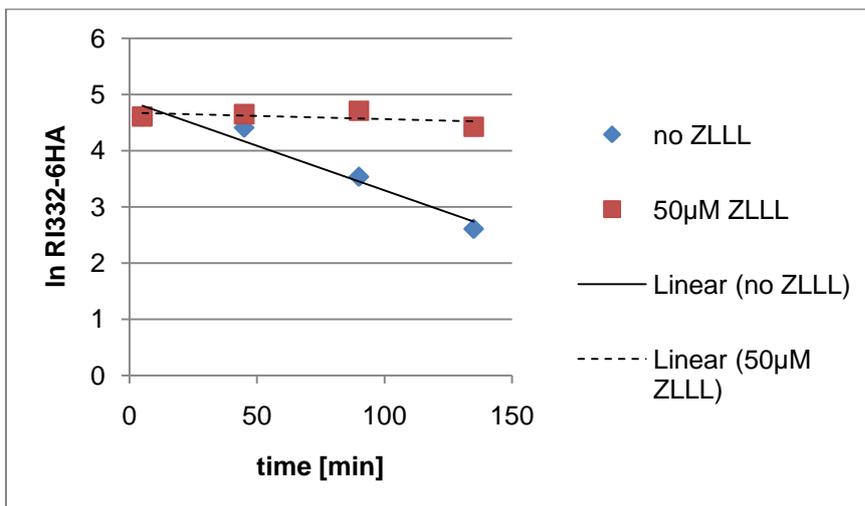
Figure 29 Determination of the half life of RI$_{332}$-6HA in QC cells (no ZLLL: squares, constant line; 50µM ZLLL: rhombs, dashed line)

No ZLLL: t$_{1/2}$= 44min

50µM ZLLL: t$_{1/2}$= 630min

Once more, ZLLL appears to exert a stronger inhibitory effect on mutant cells shifting the half life of RI$_{332}$-6HAfrom 44 minutes without inhibitor to 630 minutes with ZLLL (see figure 29). Again, intermediates of degradation of RI$_{332}$ are difficult to detect (see figure 27).

5.2.2. Analysis of the influence of dMM:

To study the effect of compromised mannose trimming on degradation, further experiments were performed applying the ER α1, 2- mannosidase inhibitor dMM. ER α1, 2- mannosidase plays a crucial role in targeting terminally misfolded proteins for ERAD by cleaving the terminal mannose in the B branch of the N-glycan. Therefore, after inhibition of this enzyme the model substrates should not be targeted for degradation, but remain within the CNX/CRT cycle. The concentration of dMM used was 2mM.

G3-RI$_{332}$ Cl. 4:
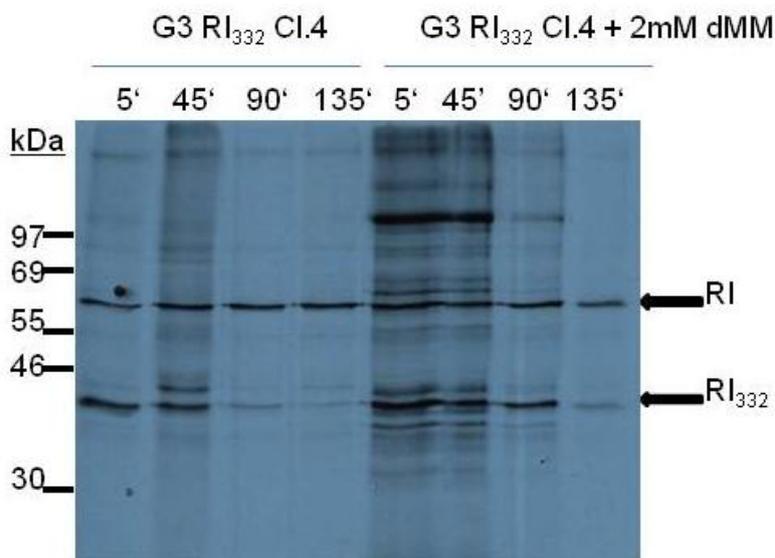
Figure 30 Fluorography of G3-RI$_{332}$ Cl. 4 ± 2mM dMM
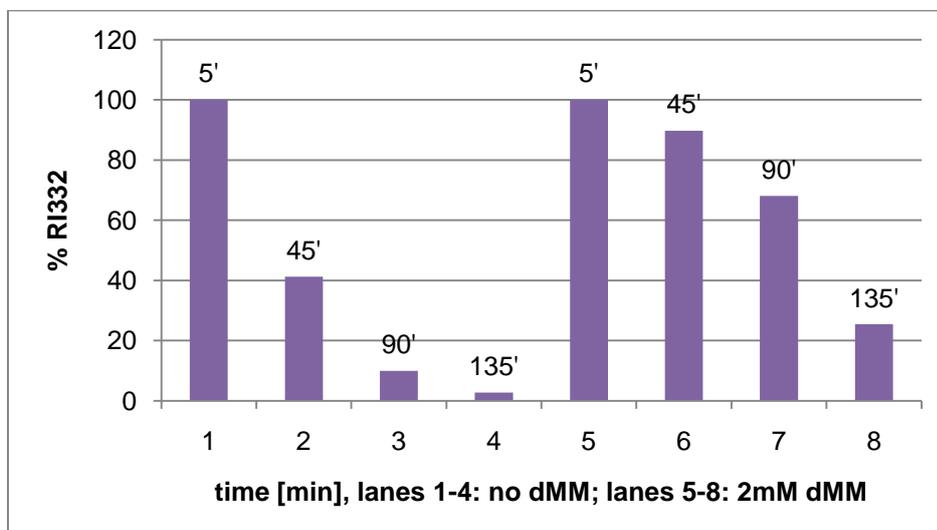
Figure 31 Degradation in G3 cells, %RI$_{332}$ during 5 to 135 minutes ± dMM
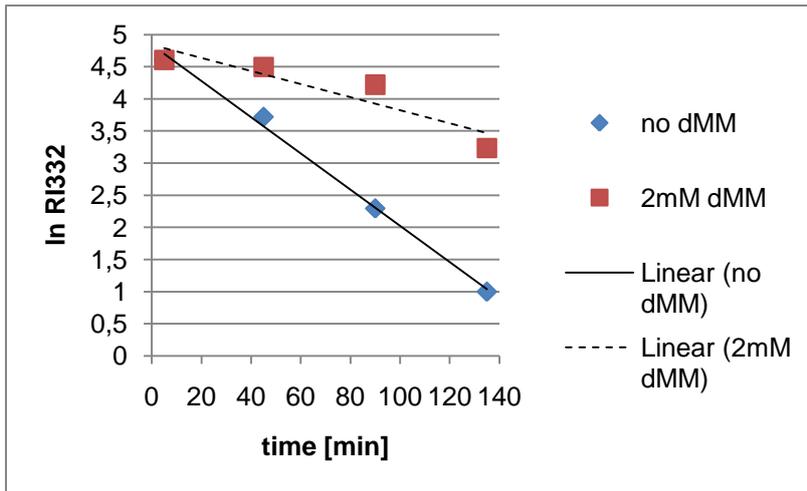
Figure 32 Determination of the half life of RI_{332} in G3 cells (no dMM: squares, constant line; 2mM dMM: rhombs, dashed line)

No dMM: $t_{1/2}$= 25min

2mM dMM: $t_{1/2}$= 68min

Inhibition with dMM leads to stabilization of the model substrate RI_{332} in wild type cells. The half life of RI_{332} without dMM was calculated to be 25 minutes, while it increases to 68 minutes upon inhibition with dMM.

QC- RI_{332} Cl.GG:
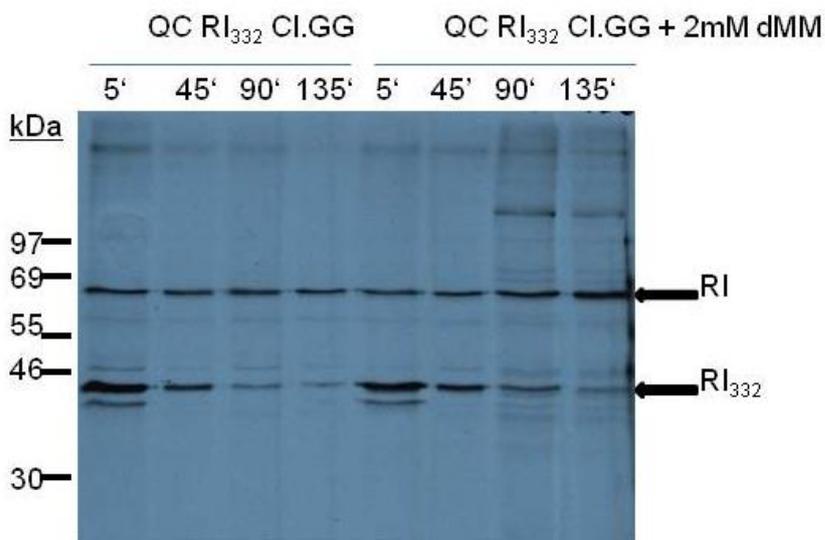
Figure 33 Fluorography of $QCRI_{332}$ Cl. GG ± 2mM dMM
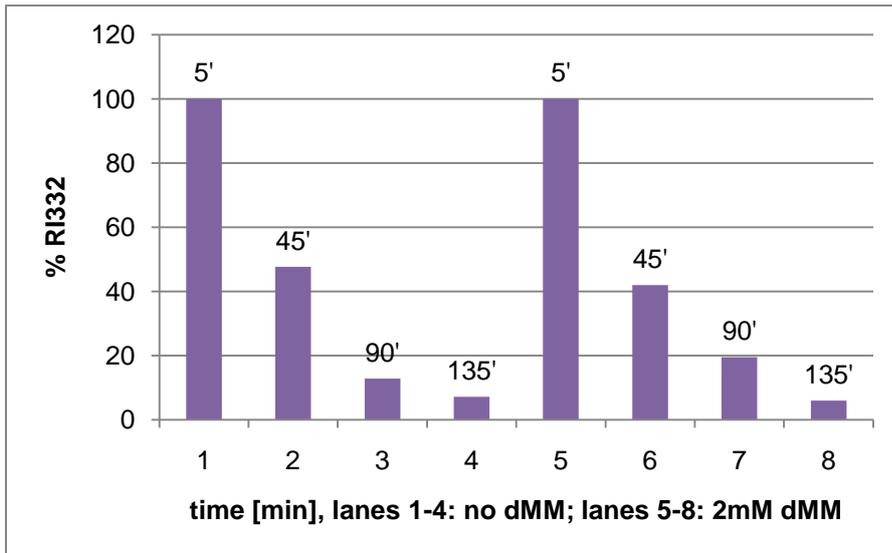
Figure 34 Degradation in QC cells, %RI_{332} during 5 to 135 minutes ± dMM
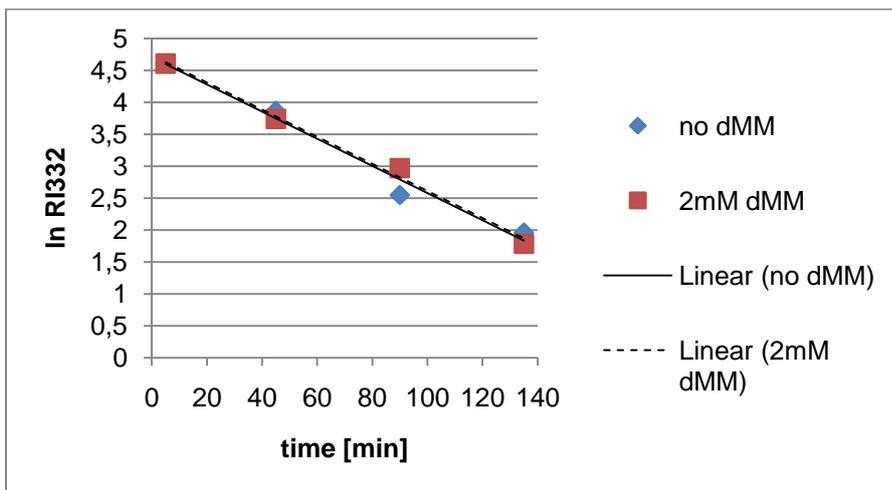
Figure 35 Determination of the half life of RI_{332} in QC cells (no dMM: squares, constant line; 2mM dMM: rhombs, dashed line)

No dMM: $t_{1/2}$= 33min

2mM dMM: $t_{1/2}$= 33min

In mutant cells expressing RI_{332} no difference between the degradation of the model substrate with and without dMM was detectable. The half life of RI_{332} without dMM as well as with dMM was determined to be 33 minutes.

<u>G3-RI$_{332}$ -6HA Cl.20:</u>
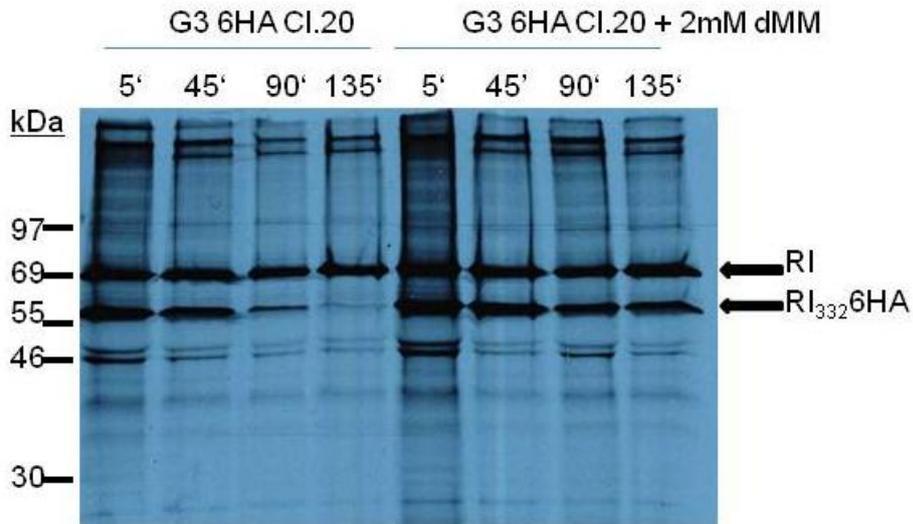
Figure 36 Fluorography of G3-RI$_{332}$ -6HA Cl. 20 ± 2mM dMM
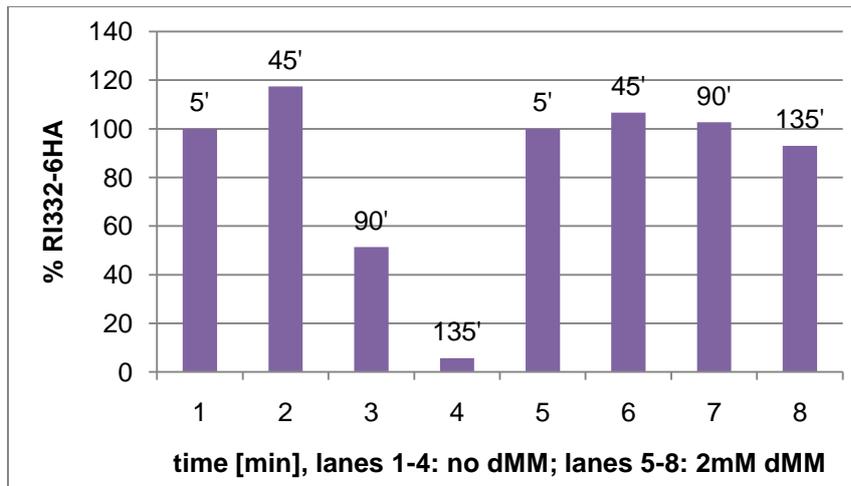
Figure 37 Degradation in G3 cells, %RI$_{332}$ -6HA during 5 to 135 minutes ± dMM
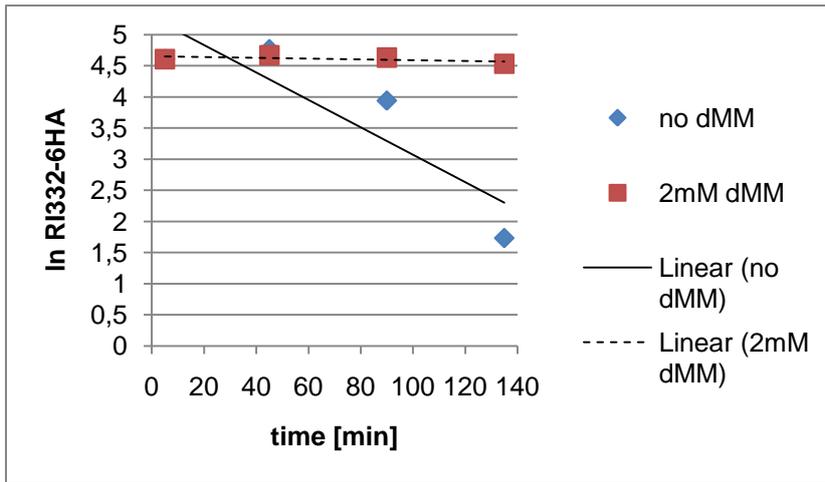
Figure 38 Determination of the half life of RI_{332}-6HA in G3 cells (no dMM: squares, constant line; 2mM dMM: rhombs, dashed line)

No dMM: $t_{1/2}$= 32min

2mM dMM: $t_{1/2}$= 1155min

Wild type cells show stabilization of the RI_{332}-6HA construct upon inhibition with dMM, with a half life shift from 32 to 1155 minutes.

QC-RI_{332} -6HA Cl.5:
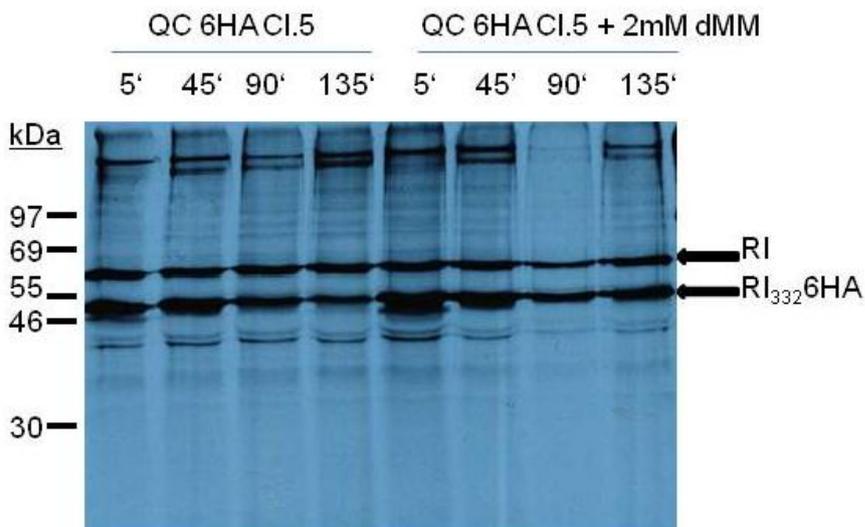
Figure 39 Fluorography of QC-RI_{332} -6HA Cl. 5 ± 2mM dMM
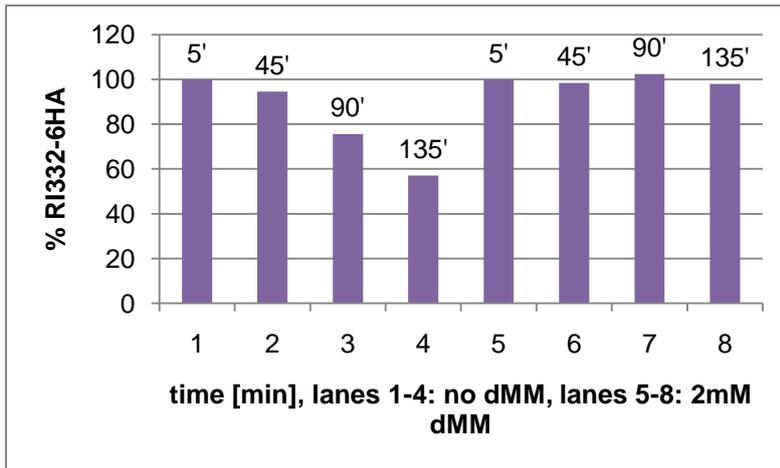
Figure 40 Degradation in QC cells, %RI$_{332}$ -6HA during 5 to 135 minutes ± dMM
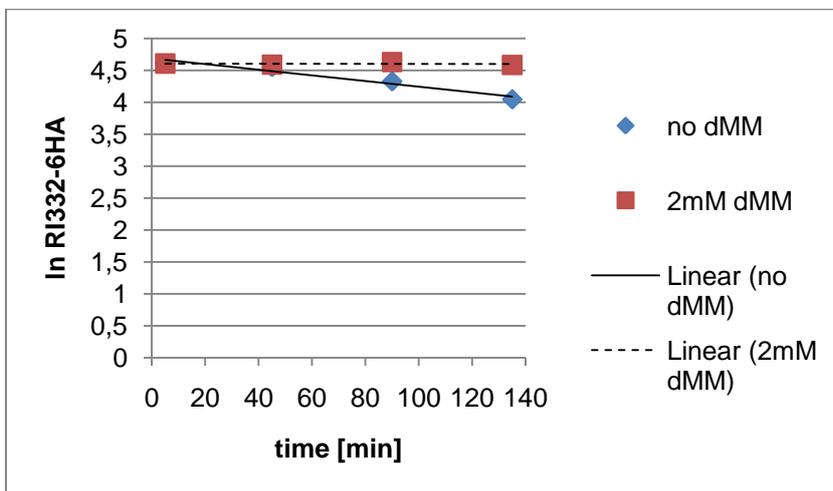
Figure 41 Determination of the half life of RI$_{332}$ -6HA in QC cells (no dMM: squares, constant line; 2mM dMM: rhombs, dashed line)

No dMM: t$_{1/2}$= 158min

2mM dMM: t$_{1/2}$= 13863min

RI$_{332}$-6HA is stabilized if dMM is applied, extending its half life from 158 minutes to 13863 minutes. Contradictory to the observations in the cell lines expressing RI$_{332}$, in cells expressing RI$_{332}$-6HA also the mutant is affected by dMM.

5.2.3. Analysis of the influence of kifunensine:

Similarly to dMM, kifunensine inhibits ER α1, 2- mannosidase and thus should lead to stabilization of the model substrates if applied. The concentration used in this assay was 2µg/ml.

Unfortunately, results were obtained only for experiments with cell lines expressing the tagged variant of RI_{332}, RI_{332}-6HA.

G3-RI_{332} -6HA Cl.20:
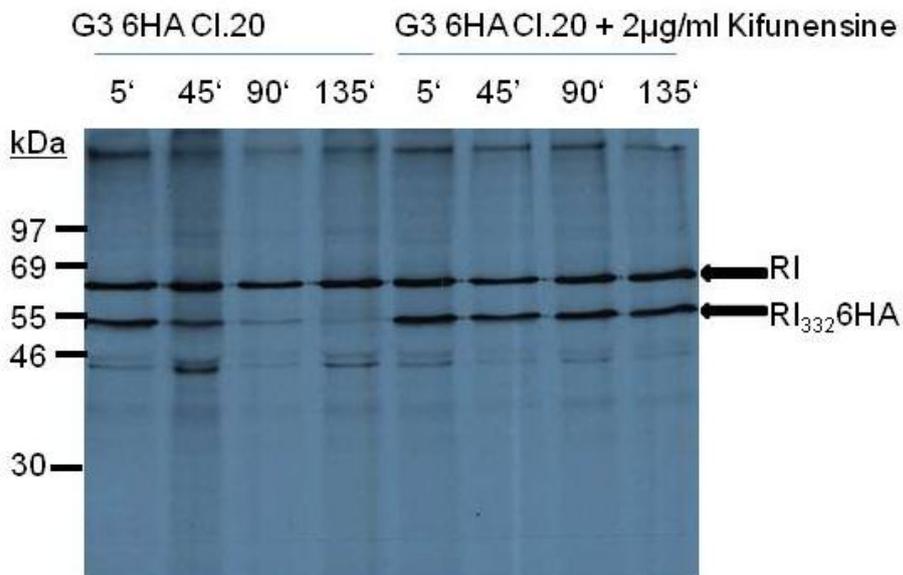
Figure 42 Fluorography of G3-RI_{332} -6HA Cl. 20 ± 2µg/ml kifunensine
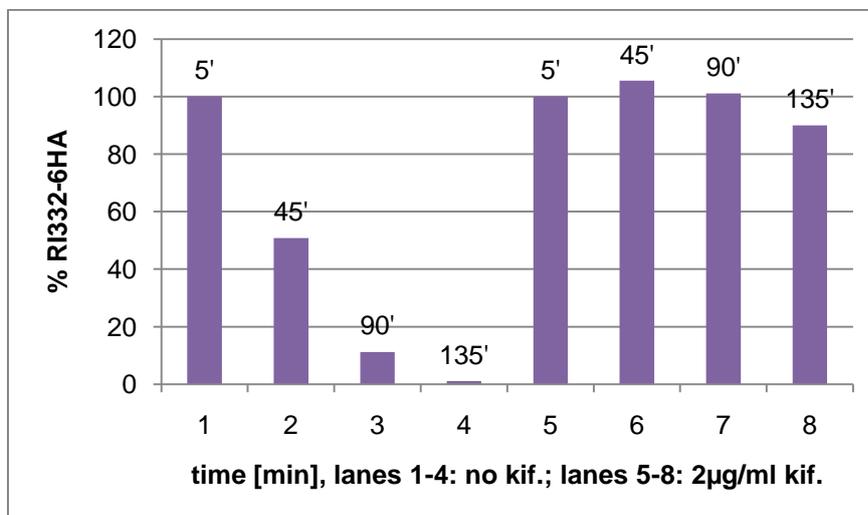
Figure 43 Degradation in G3 cells, %RI_{332} -6HA during 5 to 135 minutes ± kifunensine
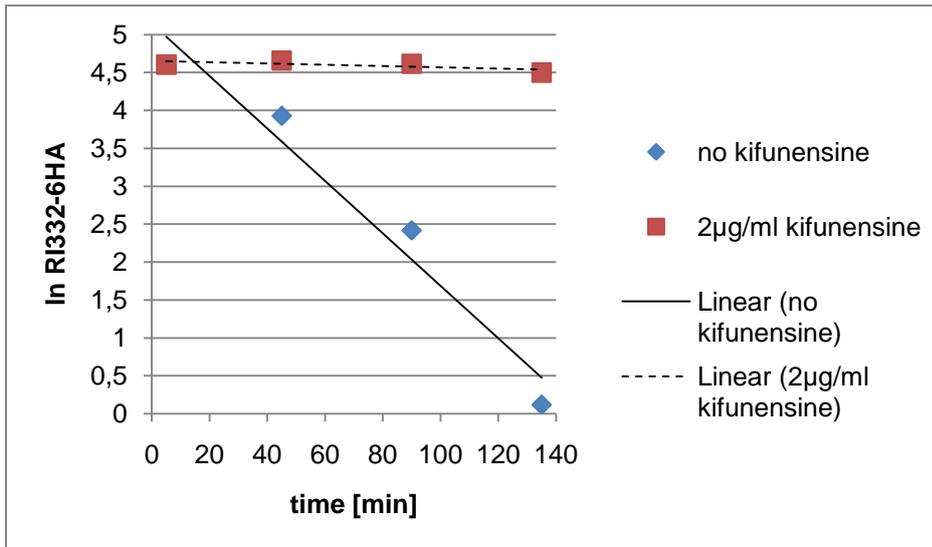
Figure 44 Determination of the half life for RI$_{332}$-6HA in G3 cells (no kifunensine: squares, constant line; 2µg/ml kifunensine: rhombs, dashed line)

No kifunensine: $t_{1/2}$= 20min

2µg/ml kifunensine: $t_{1/2}$= 770min

RI$_{332}$-6HA is stabilized through inhibition with kifunensine with the half life increasing from 20 to 770 minutes. This is consistent with the observation made with dMM in the same cell line (see 5.2.2.).

QC-RI$_{332}$ -6HA Cl.5:
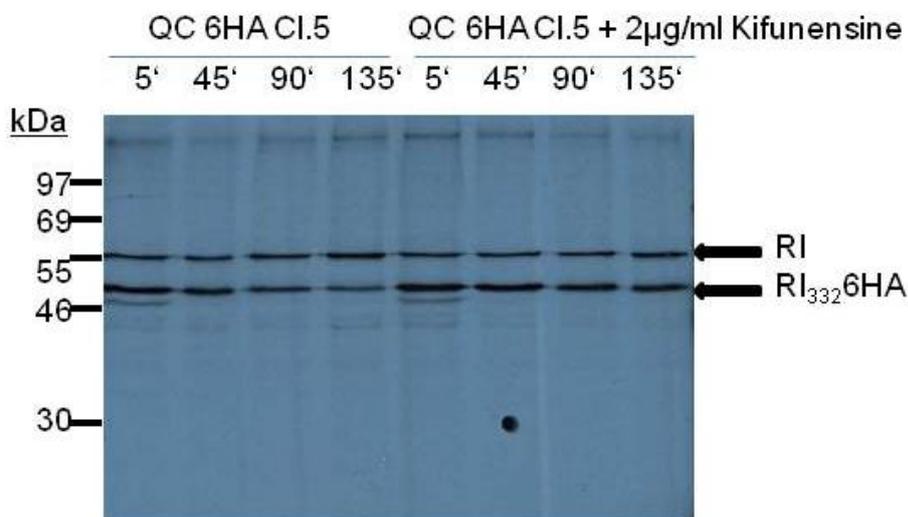
Figure 45 Fluorography of QC-RI$_{332}$ -6HA Cl. 5 ± 2µg/ml kifunensine
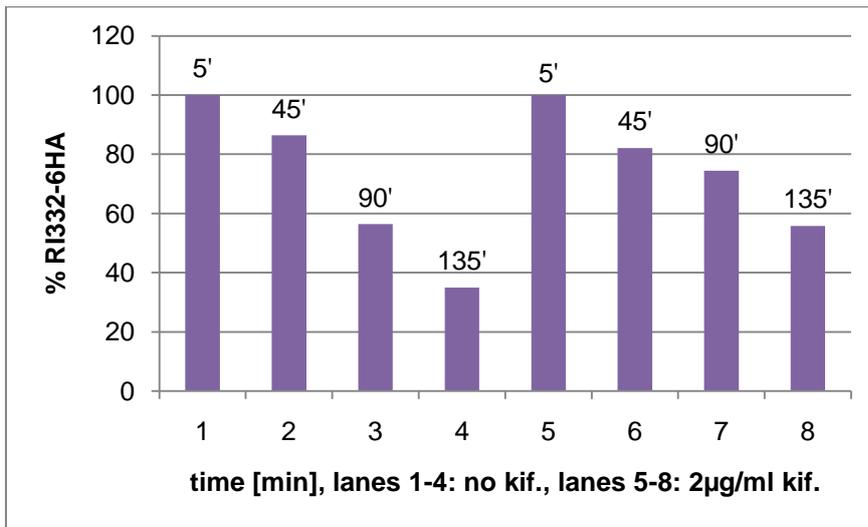
Figure 46 Degradation in QC cells, %RI$_{332}$ -6HA during 5 to 135 minutes ± kifunensine
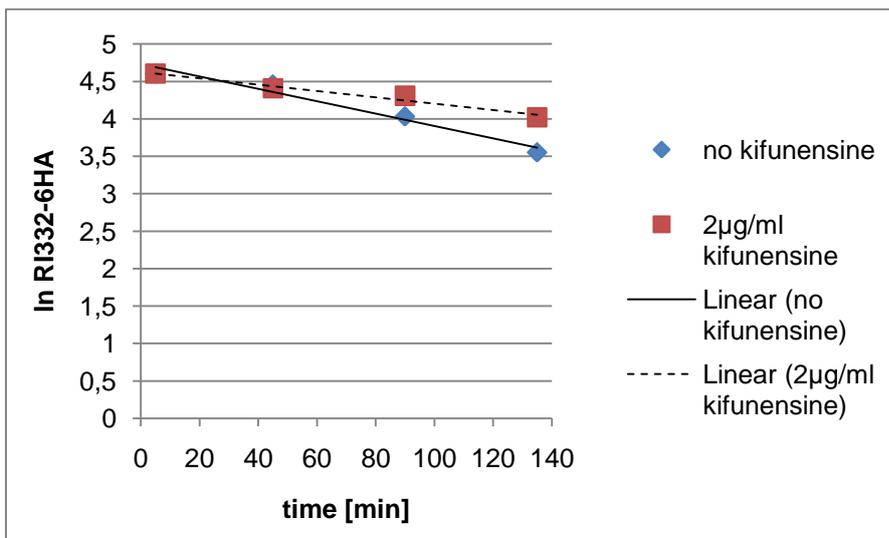
Figure 47 Determination of the half life of RI$_{332}$-6HA in G3 cells (no kifunensine: squares, constant line; 2µg/ml kifunensine: rhombs, dashed line)

No kifunensine: t$_{1/2}$= 78min

2µg/ml kifunensine: t$_{1/2}$= 144min

When kifunensine is applied to mutant cells, RI$_{332}$-6HA is stabilized, the half life shifts from 78 to 144 minutes.

5.2.4. Analysis of the influence of castanospermine:

Further, experiments applying 1mM of the inhibitor castanospermine were done. Castanospermine inhibits glucosidases I and II, enzymes responsible for targeting glycoproteins to the CNX/CRT cycle. If glucosidases I and II are not active, aberrant proteins cannot enter the CNX/CRT cycle and thus are expected to be degraded rapidly.

G3-RI$_{332}$ Cl.4:
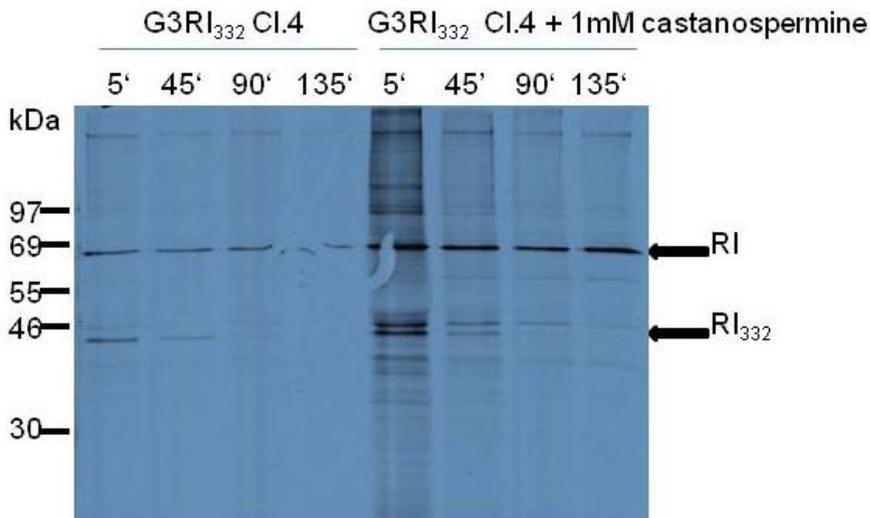
Figure 48 Fluorography of G3-RI$_{332}$ Cl.4 ± 1mM castanospermine
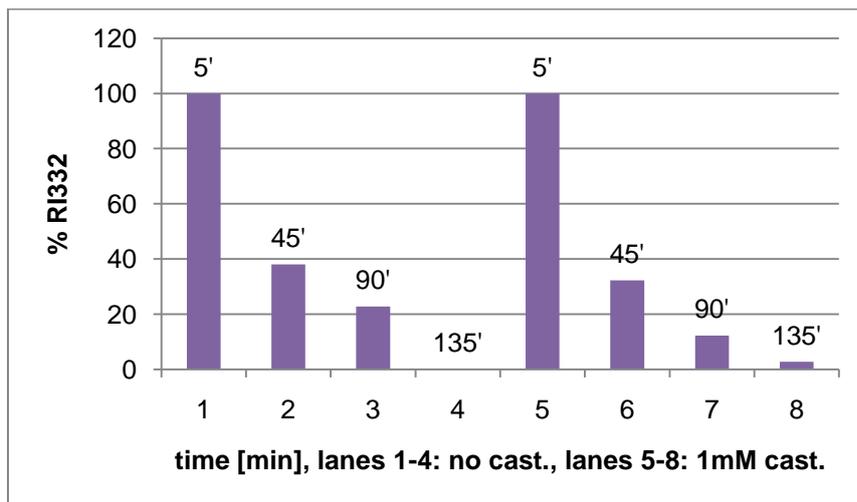
Figure 49 Degradation in G3 cells, %RI$_{332}$ during 5 to 135 minutes ± castanospermine
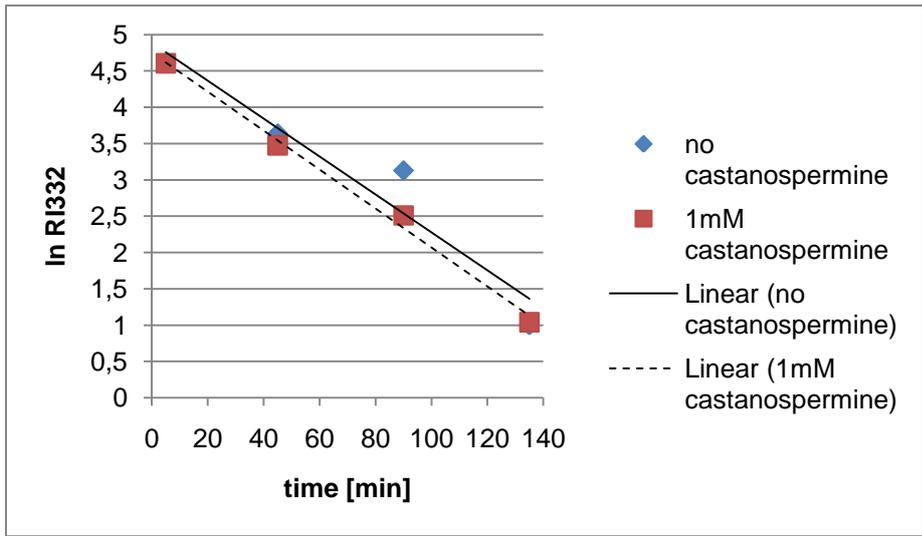
Figure 50 Determination of the half life of RI_{332} in G3 cells (no castanospermine: squares, constant line; 1mM castanospermine: rhombs, dashed line)

No castanospermine: $t_{1/2}$= 27min

1mM castanospermine: $t_{1/2}$= 26min

The influence that castanospermine exerts on $G3RI_{332}$ cells is insignificant. The half life without castanospermine was determined to be 27 minutes, with castanospermine the half life is 26 minutes.

QC-RI_{332} Cl.GG:
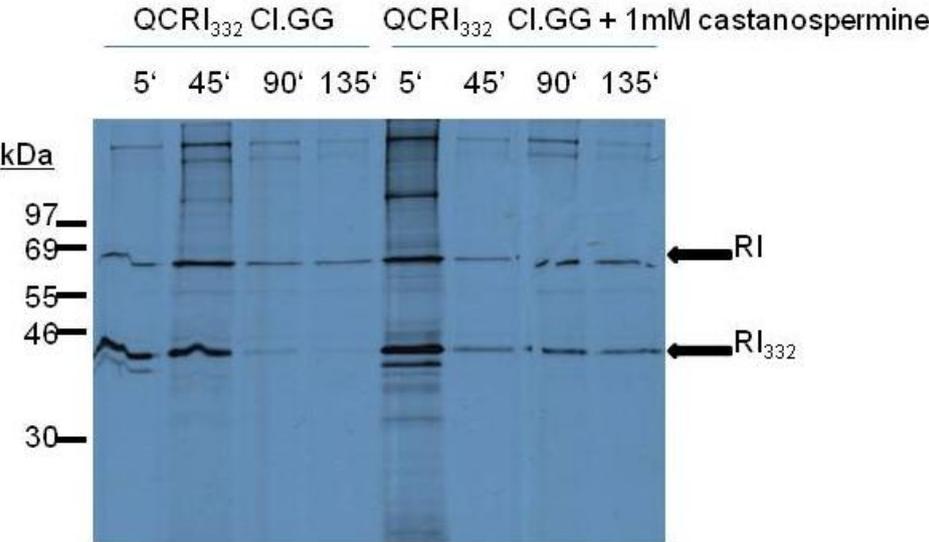
Figure 51 Fluorography of QC-RI_{332} Cl.GG ± 1mM castanospermine
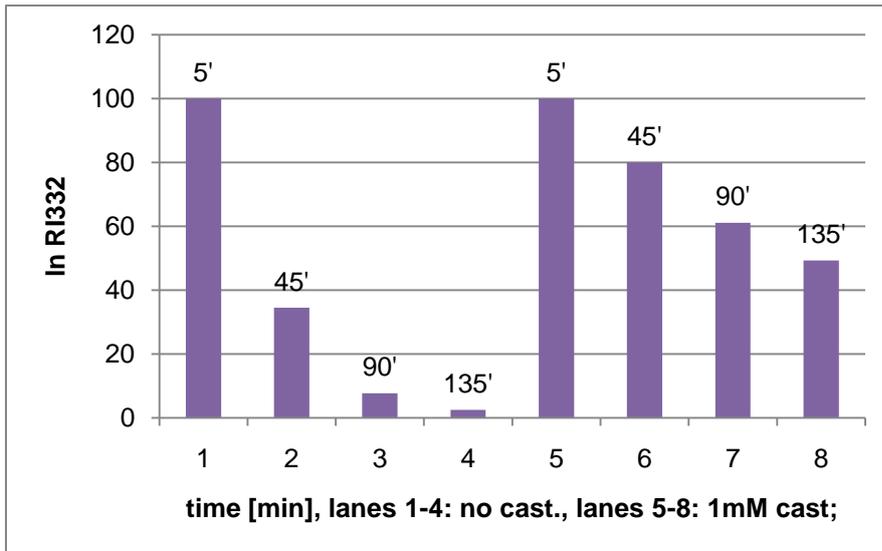
Figure 52 Degradation in QC cells, %RI_{332} during 5 to 135 minutes ± castanospermine
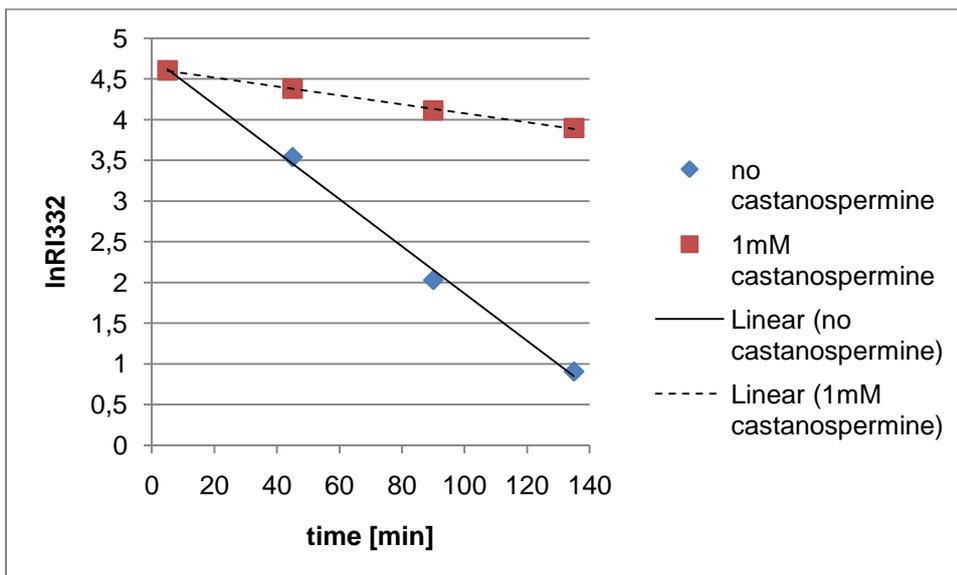
Figure 53 Determination of the half life of RI_{332} in QC cells (no castanospermine: squares, constant line; 1mM castanospermine: rhombs, dashed line)

No castanospermine: $t_{1/2}$= 24min

1mM castanospermine: $t_{1/2}$= 126min

Concerning mutant cells, RI_{332} is stabilized upon inhibition with castanospermine. The half life changes from 24 minutes to 126 minutes.

<u>G3-RI$_{332}$-6HACl.20:</u>
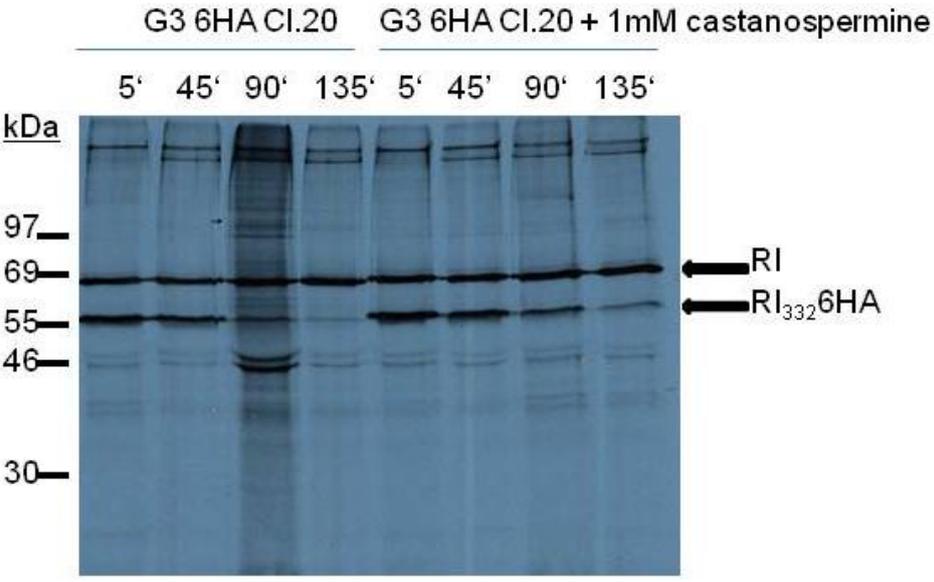
Figure 54 Fluorography of G3-RI$_{332}$-6HA Cl.20 ± 1mM castanospermine
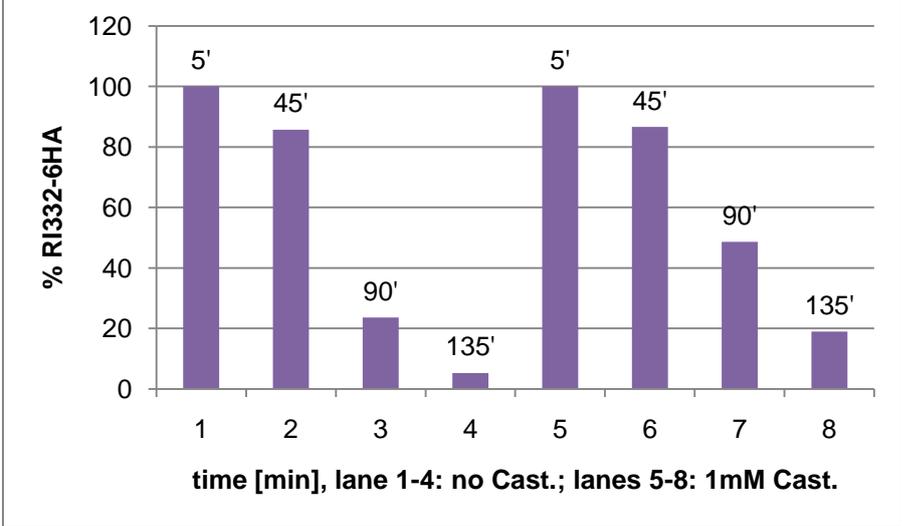
Figure 55 Degradation in G3 cells, %RI$_{332}$-6HA during 5 to 135 minutes ± castanospermine
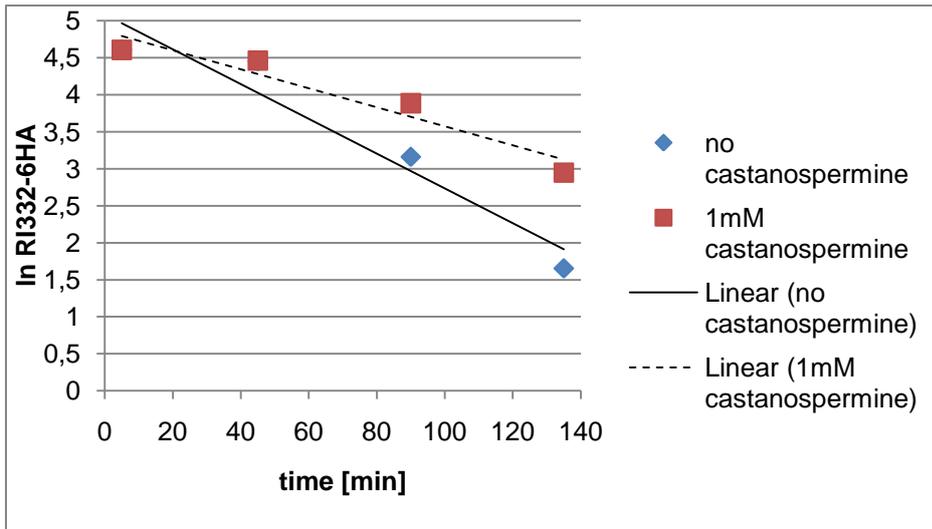
Figure 56 Determination of the half life of RI_{332}-6HA in G3 cells (no castanospermine: squares, constant line; 1mM castanospermine: rhombs, dashed line)

No castanospermine: $t_{1/2}$= 29min

1mM castanospermine: $t_{1/2}$= 54min

For $G3RI_{332}$-6HA cells, stabilization of the model protein was demonstrated when castanospermine was applied. The half life of RI_{332}-6HA rises from 29 to 54 minutes.

QC-RI_{332}-6HA Cl.5:
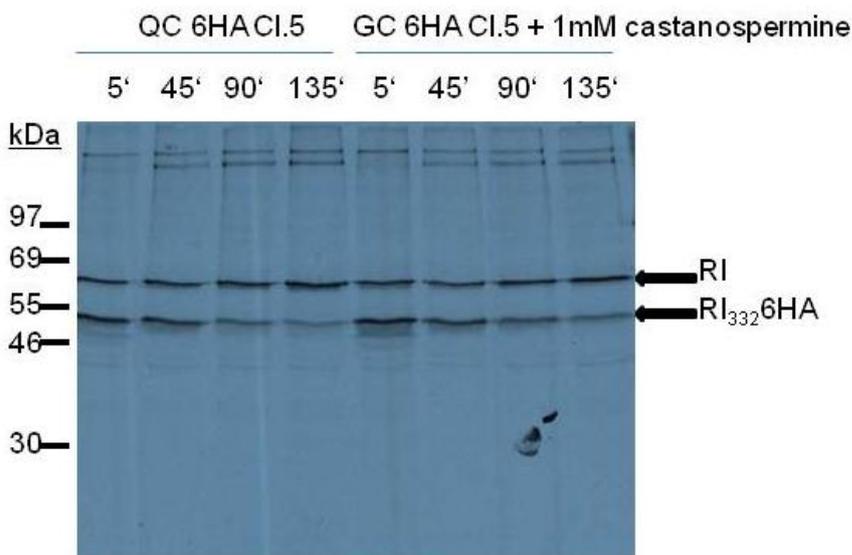
Figure 57 Fluorography of QC-RI_{332}-6HA Cl.5 ± 1mM castanospermine
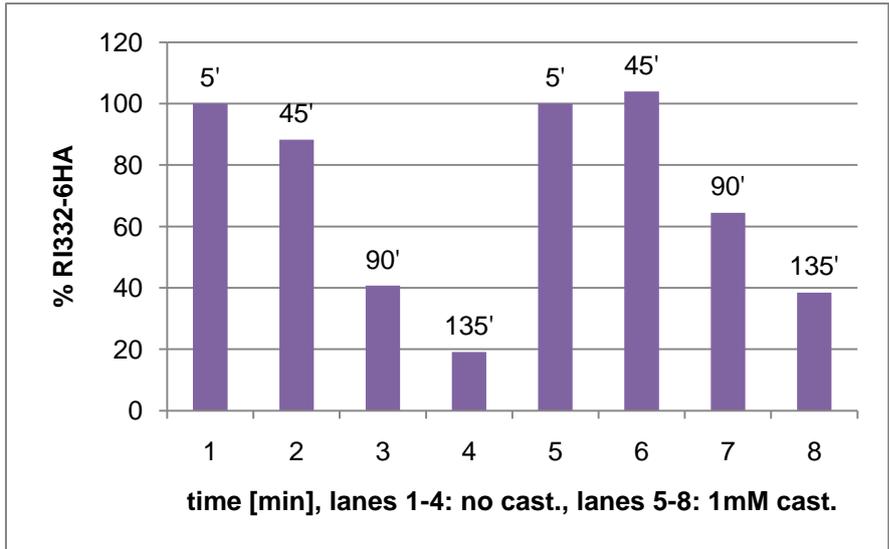
Figure 58 Degradation in QC cells, %RI_{332} -6HA during 5 to 135 minutes ± castanospermine
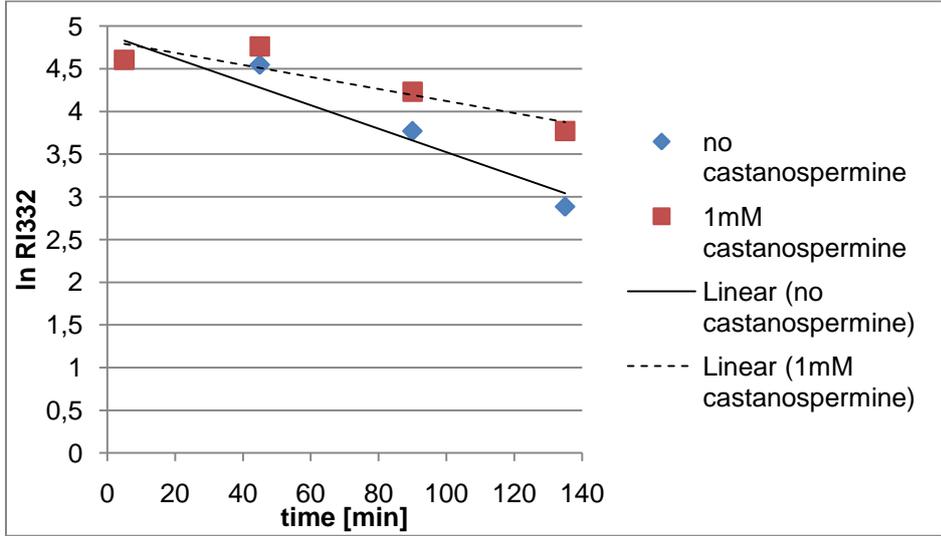
Figure 59 Determination of the half life of RI_{332}-6HA in QC cells (no castanospermine: squares, constant line; 1mM castanospermine: rhombs, dashed line)

No castanospermine: $t_{1/2}$= 51min

1mM castanospermine: $t_{1/2}$= 98min

Also in QC cells, application of the inhibitor castanospermine results in stabilization of the model substrate extending its half life from 51 to 98 minutes.

Overview of calculated half lives for the experiments performed with inhibitors:

t1/2 [min]				
	G3-RI$_{332}$ Cl.4	QC-RI$_{332}$ Cl.GG	G3-RI$_{332}$-6HA Cl.20	QC-RI$_{332}$-6HA Cl.5
control	24 ± 7 (n=5)	31 ± 15 (n=5)	28 ± 6 (n=6)	58 ± 13 (n=5)
50µM ZLLL	770	433	231	630
2mM dMM	68	33	1155	13863
1mM castanospermine	26	126	54	98
2µg/ml kifunensine	-	-	770	144

6. Discussion:

Proteins targeted for the secretory pathway pass through the endoplasmic reticulum (ER) where they undergo quality control (QC) processes. The vast majority of these proteins are glycoproteins which possess one or more N-linked glycans (GlcNAc2Man9Glc3), which are added cotranslationally. During glycoprotein folding and maturation, the N-linked glycan is trimmed by various enzymes in the lumen of the ER. Proteins playing an important role in ER quality control (ERQC) include the chaperones calnexin and calreticulin which assist during glycoprotein folding. If a protein fails to reach its native conformation, it is degraded by the ERAD pathway (Lederkremer, 2009).

 It has been shown in previous studies that UDP-glucose plays an essential role in ERQC (Hammond and Helenius, 1995). UDP-glucose is used by UGGT, an enzyme that recognizes and glucosylates misfolded glycoproteins and thus prevents them from premature degradation (Sousa and Parodi, 1995). In this study a glycosylation-deficient cell line (QC) was used which had been previously isolated and characterized in former studies (Flores-Diaz et al., 1997; 1998; 2004). Due to a mutation in the UDPG:PP gene QC cells display low levels of UDP-glucose. The control cell line (G3) used in this study represents a revertant of the mutant QC cells with wild type UDP-glucose levels. Both cell lines are stably expressing RI_{332} or RI_{332}-6HA, models for aberrant proteins interacting with the calnexin/calreticulin cycle and being substrates of the ERAD pathway. The aim of this study was to investigate the degradation of aberrant proteins in glycosylation-deficient cells compared to wild type cells. The model proteins RI_{332} and RI_{332}-6HA were expected to be degraded more rapidly in the mutant cell lines since interaction with the calnexin/calreticulin cycle should not take place (Flores-Diaz et al., 1997; 1998; 2004).

After addition of the N-glycan onto nascent polypeptides entering the ER, various enzymes participate in trimming of the oligosaccharide. They promote binding of the glycoprotein to calnexin/calreticulin, target repeatedly misfolded substrates for ERAD, ensure re-entry as well as exit from the CNX/CRT cycle (Lederkremer, 2009). To learn more about these mechanisms, experiments applying inhibitors acting on some of the key enzymes in this process were performed in G3 and QC cells.

6.1. Degradation kinetics of RI_{332} and RI_{332}-6HA in wild type and mutant cells:

In order to determine the degradation kinetics of the model substrate RI_{332} and its tagged variant RI_{332}-6HA in wild type (G3) and mutant (QC) Chinese hamster lung fibroblasts, pulse-chase experiments were performed using ^{35}S-methionine. Degradation of the model proteins

was tracked up to 120 minutes by determining relative protein amounts at different timepoints.

6.1.1. Degradation of RI$_{332}$:

Surprisingly, the degradation kinetics of the model substrate RI$_{332}$ for the wild type and the mutant cell line did not differ significantly (see figure 13). The half life of RI$_{332}$ was determined to be 13 minutes for wild type and 17 minutes for mutant cells, thus the mutant showed slightly slower degradation of the substrate protein. The half life values for G3 and QC cells determined in subsequent assays (see 6.2., controls) were higher. The mean half life of RI$_{332}$ in G3 cells was determined to be 24 ± 7 minutes and in QC cells 31 ± 15 minutes.

6.1.2. Degradation of RI$_{332}$-6HA:

For cells expressing the tagged variant of RI$_{332}$, RI$_{332}$-6HA, degradation of the substrate was found to be faster in G3 cells with a half life of 20 minutes compared to QC cells where the half life was determined to be 54 minutes. The mean half life was determined to be 28 ± 6 minutes for G3 cells and 58 ± 13 minutes for QC cells.

One reason for this unexpected behavior might be found in the tight interaction of ERAD with other cellular pathways that prevent accumulation of misfolded proteins. So for instance ERAD and UPR have been shown to be tightly linked, and an induction of molecular chaperones and enzymes might prevent aberrant proteins from preterm degradation (Vembar and Brodsky, 2008).

Studies in UDP-glucose-deficient cells demonstrated that UPR remains functionally intact, while the decrease in the cellular UDP-glucose level initiates stress signaling, which leads to overexpression of mitochondrial and ER chaperones, independently of UPR. Overexpression of six stress-induced chaperones of the ER (GRP170, GRP94, GRP78, ERp72, GRP58, and calreticulin), which participate in the maturation of proteins of the secretory pathway, has been demonstrated to be triggered in the mutant cells (Flores-Diaz et al., 2004). This modification in the expression pattern of chaperones in UDP-glucose-deficient cells could possibly lead to stabilization of the model substrates in QC cells.

6.2. Influence of inhibitors on the processing and degradation of RI_{332} and RI_{332}-6HA in wild type and mutant cells:

Moreover, pulse-chase experiments with inhibitors of proteasomal degradation, such as ZLLL as well as inhibitors of N-glycan processing, such as dMM, kifunensine and castanospermine were performed. The purpose of these experiments was to investigate the influence of these inhibitors on glycoprotein processing and degradation based on observations in preceding studies in HeLa cells (Kitzmueller et al., 2003).

Wild type (G3) and mutant (QC) cells stably expressing the proteins RI_{332} or RI_{332}-6HA were the cellular model system used in this study. After pre-incubation with an inhibitor, pulse-chase experiments were done using ^{35}S-methionine and model substrates were chased for up to 135 minutes. All media used during the labeling experiment contained inhibitor as well. In parallel, control experiments without inhibitors were performed.

6.2.1. Influence of ZLLL:

Previous studies demonstrated that RI_{332} as well as its non-glycosylated variant are effectively stabilized by inhibitors of proteasomal function, such as ZLLL. Thus, it was concluded that the degradation of these model substrates is proteasome dependent (de Virgilio et al., 1998, 1999; Kitzmueller et al., 2003).

In this study we performed pulse-chase experiments applying ZLLL to gain an insight into the degradation pathway of the model substrates RI_{332} and RI_{332}-6HA in G3 and QC cells. As expected, ZLLL could effectively stabilize the model substrates in all four clones. The half life of RI_{332} for G3 cells was determined to be 31 minutes without and 770 minutes with ZLLL (see figure 20). The half life of the same substrate in QC cells rose from 55 minutes without to 433 minutes with the inhibitor (see figure 23). Addition of ZLLL to G3 cells expressing RI_{332}-6HA led to an increase in the half life from 30 minutes to 231 minutes (see figure 26). For QC cells expressing RI_{332}-6HA, the half life was calculated to rise from 44 minutes without to 630 minutes with ZLLL.

Two additional bands could be detected just underneath the band representing RI_{332} in ZLLL-treated G3 and QC cells expressing RI_{332}. Based on former studies (Kitzmueller et al., 2003), the bands could represent degradation intermediates of RI_{332}, one glycosylated (RI_{332}i1), one un-glycosylated (RI_{332}i2) (see figures 18 and 21).

6.2.2. Influence of dMM:

ER α1, 2- mannosidase plays an essential role in targeting terminally misfolded proteins for ERAD. It cleaves the terminal mannose in the B branch of N-glycans and thus promotes the exit from the CNX/CRT cycle of glycoproteins (Helenius et al., 2005). Former studies revealed the central role of ER α1, 2- mannosidase in the initial steps of protein degradation. Experiments performed in murine heptoma cells demonstrated the influence of the concentration of ER α1, 2- mannosidase on the degradation of the AAT (alpha-1 antitrypsin) protein. Elevated ER α1, 2- mannosidase activity led to enhanced destabilization of the AAT protein, whereas application of kifunensine, a general α1, 2- mannosidase inhibitor, resulted in stabilization of the protein of interest. Overexpression of ER α1, 2- mannosidase was demonstrated to lead to accelerated degradation of ERAD substrates and increased trimming of mannose residues (Wu et al., 2003). Further, knockdown of ER α1, 2- mannosidase was shown to dramatically stabilize ERAD substrates (Avezov et al., 2008).

To gain an insight into the targeting of glycoproteins for ERAD in wild type and glycosylation-deficient cells, the ER α1, 2- mannosidase inhibitor dMM was applied and pulse-chase experiments were performed. Since RI_{332} and RI_{332}-6HA should remain within the CNX/CRT cycle upon inhibition with dMM, the model substrates were expected to be stabilized.

For G3 cells, dMM was able to stabilize the model proteins. The calculated half lives for RI_{332} were 25 minutes without and 68 minutes with the inhibitor in wild type cells (see figure 32). For RI_{332}-6HA the half life was determined to shift from 32 minutes without dMM to 1155 minutes with dMM (see figure 38). For QC cells expressing RI_{332}-6HA, the model substrate was shown to be stabilized as well with the unusuallly high half life of 158 minutes without inhibitor and 13863 minutes with dMM (see figure 41). QC celllls expressing RI_{332} did not show any differences between dMM-treated and control cells. The calculated half life was 33 minutes for both experiments (see figure 35).

One explanation why QC cell expressing RI_{332} were not influenced by dMM could be, that in mutant cells, due to the lack of glucosylation, the model proteins do not enter the CNX/CRT cycle at all and are therefore rapidly degraded. Still, for QC cells expressing RI_{332}-6HA, the model substrate appears to be stabilized. This discrepancy needs to be clarified in further work.

6.2.3. Influence of kifunensine:

Just like dMM, kifunensine represents an inhibitor of ER α1, 2- mannosidase (Wu et al., 2003). Thus, pulse-chase experiments performed with kifunensine were expected to lead to stabilization of the model proteins, at least in wild type cells.

Unfortunately, results were obtained only for experiments with cell lines expressing the tagged variant of RI_{332}, i.e. G3 RI_{332}-6HA Cl.20 and QC RI_{332}-6HA Cl.5.

As expected, degradation of the model substrate RI_{332}-6HA was inhibited by the application of kifunensine. The half lives were determined to be 20 minutes for RI_{332}-6HA in wild type cells without and 770 minutes with kifunensine (see figure 44). The half lives calculated for the model protein in mutant cells were 78 minutes without and 144 minutes with the inhibitor. Thus, the effect of inhibition by kifunensine in QC cells was less apparent than in G3 cells.

6.2.4. Influence of castanospermine:

Experiments using the inhibitor castanospermine were performed, as castanospermine is known to inhibit glucosidases I and II, enzymes responsible for removal of the outer two glucose moieties of the N-glycan (Palamarczyk and Elbein, 1985). Glycoproteins possessing monoglucosylated N-glycans are able to enter the CNX/CRT cycle, which supports correct folding. If glucosidases I and II are blocked, aberrant proteins should not be able to enter the CNX/CRT cycle and be degraded rapidly instead. By application of castanospermine, destabilization, i.e. faster degradation of RI_{332} and RI_{332}-6HA, was expected.

Experiments in cell-free systems such as the study performed in a mammalian semipermeabilised cell system treated with castanospermine, resulted in faster degradation of class I major histocompatibility complex (MHC) heavy chains (Wilson et al., 2000).

Nevertheless, for G3 cells expressing RI_{332} the half lives were determined to be 27 minutes without and 26 minutes with castanospermine (see figure 50). Generally, it has to be mentioned that difficulties were encountered concerning this clone. G3-RI_{332} Cl.4 cells lost expression of the RI_{332}-construct repeatedly. Therefore, this experiment should be repeated with another clone of G3 cells expressing RI_{332}.

For the mutant cell line expressing RI_{332} half lives of RI_{332} were 24 minutes without and 126 minutes with the inhibitor (see figure 53). Also for the cell lines expressing RI_{332}-6HA half lives for the model protein rose if castanospermine was applied. RI_{332}-6HA in wild type cells had a half life of 29 minutes without and 54 minutes with castanospermine (see figure 56).

For mutant cells, calculated half lives were 51 minutes for control experiments and 98 minutes for experiments carried out with castanospermine (see figure 59).

An inhibitory effect of castanospermine on the degradation of misfolded proteins has been demonstrated in former studies. Experiments in cells transfected with the NHK (null Hong Kong) protein, a genetic variant of AAT and substrate of the ERAD pathway, indicated a modest inhibitory effect on NHK degradation upon inhibition with castanospermine (Oda et al., 2003). This is consistent with the results of additional experiments, such as studies investigating the degradation of the Ig subunits μ, J, and λ in assembly-deficient myeloma transfectants. Although it was demonstrated that μ-chains did not bind to calnexin after inhibition with castanospermine, the inhibitor had only little or no effect on the degradation of μ- and J-chains (Fagioli and Sitia, 2001). Moreover, experiments in Chinese hamster ovary (CHO) cells expressing the cog thyroglobulin (Tg) mutant, a misfolded glycoprotein serving as a model for ER storage diseases, demonstrated that suppression of ERAD with inhibitors of ER α1, 2- mannosidase was efficient in cells treated with castanospermine (Tokunaga et al., 2000). Thus, the authors concluded that chaperones other than calnexin and calreticulin might have as well the potential to participate in retaining misfolded proteins within the ER and targeting them for ERAD.

6.3. Summary and Outlook:

Taken together, experiments determining the degradation kinetics of the model substrates RI_{332} and RI_{332}-6HA revealed that, contrary to all expectations, RI_{332} or RI_{332}-6HA were not degraded faster in glucosylation-deficient cells. Instead, determined half lives for cells expressing RI_{332} were almost the same for mutant and wild type cells. Concerning the cells expressing RI_{332}-6HA, mutant cells even showed slower degradation of the model protein, almost doubling the half life of RI_{332}-6HA. The reasons for this unexpected behavior could lie within the interaction of the model proteins with ER chaperones, which have been shown to be overexpressed in UDP-glucose-deficient cells in former studies (see above, Flores-Diaz et al., 2004). As expected, the endogenous protein ribophorin I remained stable during all chase times.

Regarding experiments performed with inhibitors, inhibition of proteasomal degradation of RI_{332} or RI_{332}-6HA was observed by application of ZLLL. In all cell lines the model proteins were strongly stabilized by proteasomal inhibition, demonstrating that RI_{332} and RI_{332}-6HA are substrates of the ERAD pathway. Inhibition of ER α1, 2- mannosidase by dMM or kifunensine led to controversial results. For cells expressing RI_{332}, application of dMM stabilized the model substrate in G3 cells, but not in QC cells, while half lives for the model substrates of

the clones expressing RI_{332}-6HA rose tremendously with QC cells displaying an unusually high value. Experiments performed with kifunensine as well showed stabilization of RI_{332}-6HA for wild type and mutant cells, although stabilization was stronger for G3 cells. Unfortunately, no results were obtained concerning kifunensine inhibition of cells expressing RI_{332}. Altogether, inhibition of ER α1, 2- mannosidase was demonstrated to lead to stabilization of the model proteins, at least in wild type cells. Concerning mutant cells, glucosylation-deficiency might prevent the entry of RI_{332} or RI_{332}-6HA into the CNX/CRT cycle and lead to rapid degradation of the model substrates, thus impeding the action of dMM or kifunensine. Expecting destabilization of RI_{332} or RI_{332}-6HA, experiments applying the inhibitor castanospermine were performed. Surprisingly, castanospermine showed to exhibit no or contrary effect on wild type cells, not influencing the stability of RI_{332}, but stabilizing RI_{332}-6HA in G3 cells. Furthermore, RI_{332} and RI_{332}-6HA were stabilized in mutant cells. Similar observations have been made in former studies (see above) leading to the assumption that pathways other than the CNX/CRT cycle must be involved in retention of misfolded proteins in the ER as well as in targeting these proteins for ERAD.

To learn more about the effects of the inhibitors dMM, kifunensine and castanospermine on the interaction of RI_{332} and RI_{332}-6HA with the CNX/CRT cycle, and to see if such an interaction occurs at all, co-immunoprecipitation experiments using antibodies for the model substrates as well as antibodies for calnexin and/or calreticulin will have to be performed. Besides inhibition experiments with dMM and kifunensine, knockdown of ER α1, 2- mannosidase by RNA interference might help to gain an insight into the role of this enzyme in the ERAD pathway in wild type and glucosylation-deficient Chinese hamster fibroblasts.

7. Abbreviations:

ALG	Asparagine-linked glycosylation
ATF6	Activating Transcription Factor-6
BiP	Binding Protein
CDG	Congenital Disorders of Glycosylation
CNX	Calnexin
COP	Coat Protein Complex
CRT	Calreticulin
dMM	Deoxy-mannojirimycin
EDEM	ER degradation enhancing 1, 2-mannosidase-like protein
eIF2α	Eukaryotic Translation Initiation Factor-2
ER	Endoplasmic Reticulum
ERAD	ER-associated degradation
ERES	ER Exit Site
ERGIC	ER-Golgi Intermediate Compartment
ERp72	ER protein 72
Glc	Glucose
GlcNAc	N-acetylglucosamine
GRP	Glucose-regulated protein
GPI	Glycophosphatidylinositol
GRP 94	Glucose-regulated protein 94
HA	Hemagglutinin
Ig	Immunoglobulin
IRE1	Inositol-requiring Protein-1
Man	Mannose
OST	Oligosaccharyltransferase
PDI	Protein Disulphide Isomerase
QC	Quality Control
RAP	Receptor-associated protein
RI	Ribophorin I
Tg	Thyroglobulin
UDPG:PP	Uridine Diphosphate Glucose:Pyrophosphorylase
UGGT	UDP-glucose:glycoprotein glycosyltransferase

UPR	Unfolded Protein Response
UPRE	UPR Element
ZLLL	Carbobenzoxy-l-leucyl-l-leucyl-l-leucinal

8. References:

Anelli T.and Sitia R. 2008. Protein quality control in the early secretory pathway. EMBO J. 27 315–327.

Arnold SM, Fessler LI, Fessler JH, Kaufman RJ 2000. Two homologues encoding human UDP-glucose:glycoprotein glucosyltransferase differ in mRNA expression and enzymatic activity. Biochemistry 39: 2149–2163.

Avezov E, Frenkel Z, Ehrlich M, Herscovics A, Lederkremer GZ. 2008. Endoplasmic Reticulum (ER) Mannosidase I Is Compartmentalized and Required for N-Glycan Trimming to Man5 6GlcNAc2 in Glycoprotein ER-associated Degradation. Mol Biol Cell. 2008;19:216–225.

Barlowe C. 2002. COPII-dependent transport from the endoplasmic reticulum. Curr Opin Cell Biol 14:417–422

Barlowe, C. 2003. Signals for COPII-dependent export from the ER: what's the ticket out? Trends Cell Biol. 13 295-300.

Bateman D., 2006, Unfolded Protein Response (UPR): Cellular control for our errors in life. Hypothesis 2006, Vol 4, No 1; 33-37.

Buschhorn, B.A., Z. Kostova, B. Medicherla, and D.H. Wolf. 2004. A genome-wide screen identifies Yos9p as essential for ER-associated degradation of glycoproteins. FEBS Lett. 577:422–426.

Caramelo JJ, Parodi AJ. 2008. Getting in and out from calnexin/calreticulin cycles. J Biol Chem. 2008;283:10221–5.

Caramelo, J. J., Castro, O. A., Alonso, L. G., de Prat-Gay, G., and Parodi, A. J. 2003. UDP-Glc:glycoprotein glucosyltransferase recognizes structured and solvent accessible hydrophobic patches in molten globule-like folding intermediates.Proc. Natl. Acad. Sci. U. S. A. 100 86–91.

Casagrande R., Stern P., Diehn M., Shamu C., Osario M., Zuniga M., Brown P. O., Ploegh H. 2000. Degradation of proteins from the ER of S. cerevisiae requires an intact unfolded protein response pathway. Mol. Cell. 2000;5:729–735.

Christianson J.C., Shaler T.A., Tyler R.E., Kopito R.R. 2008. OS-9 and GRP94 deliver mutant alpha1-antitrypsin to the Hrd1-SEL1L ubiquitin ligase complex for ERAD. Nat. Cell Biol. 2008;10:272–282. doi: 10.1038/ncb1689.

Clerc S., Hirsch C., Oggier D. M., Deprez P., Jakob C., Sommer T., Aebi M. 2009. Htm1 protein generates the N-glycan signal for glycoprotein degradation in the endoplasmic reticulum. J. Cell Biol. 2009;184:159–172.

Danilczyk UG, Cohen-Doyle MF, Williams DB. 2000. Functional relationship between calreticulin, calnexin, and the endoplasmic reticulum luminal domain of calnexin. J Biol Chem. 2000;275:13089–13097.

de Virgilio, M., Kitzmuller, C., Schwaiger, E., Klein, M., Kreibich, G. and Ivessa, N. E. 1999. Degradation of a short-lived glycoprotein from the lumen of the endoplasmic reticulum: the role of N-linked glycans and the unfolded protein response. Mol. Biol. Cell 10, 4059–4073.

de Virgilio, M., Weninger, H., and Ivessa, N. E. 1998. Ubiquitination is required for the retro-translocation of a short-lived luminal endoplasmic reticulum glycoprotein to the cytosol for degradation by the proteasome. J. Biol. Chem. 273 9734–9743.

Deprez, P., Gautschi, M., and Helenius, A. 2005. More Than One Glycan Is Needed for ER Glucosidase II to Allow Entry of Glycoproteins into the Calnexin/Calreticulin Cycle. Mol. Cell 19 183-195.

Ellgaard L., Helenius A. 2003. Quality control in the endoplasmic reticulum. Nat. Rev. Mol. Cell Biol. 2003;4:181–191.

Ellgaard L., Molinari M., Helenius A. 1999. Setting the standards: quality control in the secretory pathway. Science. 1999;286:1882–1888.

Ellgaard L., Riek R., Herrmann T., Guntert P., Braun D., Helenius A., Wuthrich K. 2001. NMR structure of the calreticulin P-domain. Proc. Natl. Acad. Sci. USA. 2001;98:3133–3138.

Ermonval M., Kitzmuller C., Mir A. M., Cacan R., Ivessa N. E. 2001. N-glycan structure of a short-lived variant of ribophorin I expressed in the MadIA214 glycosylation-defective cell line reveals the role of a mannosidase that is not ER mannosidase I in the process of glycoprotein degradation. Glycobiology. 2001; 11:565–576.

Fagioli C, Sitia R. Glycoprotein quality control in the endoplasmic reticulum. Mannose trimming by endoplasmic reticulum mannosidase I times the proteasomal degradation of unassembled immunoglobulin subunits. 2001. J. Biol. Chem. 2001;276:12885–12892.

Flores-Díaz M, Alape-Girón A, Titball RW, Moos M, Guillouard I, Cole S, Howells AM, von Eichel-Streiber C, Florin I, Thelestam M. UDP-glucose deficiency causes hypersensitivity to the cytotoxic effect of Clostridium perfringens phospholipase C. J Biol Chem. 1998 Sep 18;273(38):24433–24438.

Flores-Diaz M, Higuita JC, Florin I, Okada T, Pollesello P, Bergman T, Thelestam M, Mori K, Alape-Giron A. 2004. A cellular UDP-glucose deficiency causes overexpression of glucose/oxygen-regulated proteins independent of the endoplasmic reticulum stress elements. J Biol Chem. 2004;279:21724–21731.

Flores-Diaz, M., A. Alape-Giron, B. Persson, P. Pollesello, M. Moos, C. von Eichel-Streiber, M. Thelestam, and I. Florin. 1997. Cellular UDP-glucose deficiency caused by a single point mutation in the UDP-glucose pyrophosphorylase gene. J. Biol. Chem. 272:23784-23791.

Florin I. 1991. Isolation of a fibroblast mutant resistant to Clostridium difficile toxin B. Microbial Pathogenesis. 1991;11:337–346. 10.1016/0882-4010(91)90019-7.

Freeze H., Jeffrey D. Esko, and Armando J. Parodi. 1999. Glycans in Glycoprotein Quality Control. Essentials of Glycobiology, 2nd Edition, 1999.

Freeze HH, Aebi M. 2005. Altered glycan structures: The molecular basis of congenital disorders of glycosylation. Curr Opin Struct Biol. 2005;15:490–498.

Frickel E. M., Frei P., Bouvier M., Stafford W. F., Helenius A., Glockshuber R., Ellgaard L. 2004. ERp57 is a multifunctional thiol-disulfide oxidoreductase. J. Biol. Chem. 2004;279:18277–18287.

Frickel E. M., Riek R., Jelesarov I., Helenius A., Wuthrich K., Ellgaard L. 2002. TROSY-NMR reveals interaction between ERp57 and the tip of the calreticulin P-domain. Proc. Natl. Acad. Sci. USA. 2002;99:1954–1959.

Friedlander R, Jarosch E, Urban J, Volkwein C, Sommer T. 2000. A regulatory link between ER-associated protein degradation and the unfolded-protein response. Nat Cell Biol 2:379–384.

Gauss, R., E. Jarosch, T. Sommer, and C. Hirsch. 2006. A complex of Yos9p and the HRD ligase integrates endoplasmic reticulum quality control into the degradation machinery. Nat. Cell Biol. 8:849–854.

Ghaemmaghami S, et al. 2003. Global analysis of protein expression in yeast. Nature. 2003;425(6959):737–741.

Haigh N., Johnson A. 2002. A new role for BiP: closing the aqueous translocon pore during protein integration into the ER membrane. J. Cell Biol. 2002;156:261–270.

Hammond C, Helenius A. 1995. Quality control in the secretory pathway. Curr. Opin. Cell Biol. 1995;7:523–529.

Harnik-Ort, V., K. Prakash, E. Marcantonio, D.R. Colman, M.G. Rosenfeld, M. Adesnik, D.D. Sabatini, and G. Kreibich. 1987. Isolation and characterization of cDNA clones for rat ribophorin I: complete coding sequence and in vitro synthesis and insertion of the encoded product into endoplasmic reticulum membranes. J. Cell Biol. 104:855–863.

Harris MR, Yu YY, Kindle CS, Hansen TH, Solheim JC. 1998. Calreticulin and calnexin interact with different protein and glycan determinants during the assembly of MHC class I. J Immunol. 1998;160:5404–9.

Hebert, D. N., Zhang, J. X., Chen, W., Foellmer, B., and Helenius, A. 1997. The Number and Location of Glycans on Influenza Hemagglutinin Determine Folding and Association with Calnexin and Calreticulin J. Cell Biol. 139 613-623.

Helenius A, Aebi M.2001. Intracellular functions of N-linked glycans. Science. 2001;291:2364–2369. doi: 10.1126/science.291.5512.2364.

Helenius, A., E. S. Trombetta, D. N. Hebert, and J. F. Simons. 1997. Calnexin, calreticulin and the folding of glycoproteins. Trends Cell Biol. 7193-200.

Herrmann, J.M., P. Malkus, and R. Schekman. 1999. Out of the ER–outfitters, escorts and guides. Trends Cell Biol. 9:5–7.

Kanapin A, Batalov S, Davis MJ, Gough J, Grimmond S, Kawaji H, Magrane M, Matsuda H, Schonbach C, Teasdale RD, et al. 2003. Mouse proteome analysis. Genome Res. 2003;13:1335–1344.

Kanehara, K., S. Kawaguchi, and D.T. Ng. 2007. The EDEM and Yos9p families of lectin-like ERAD factors. Semin. Cell Dev. Biol. 18:743–750.

Keith N, Parodi AJ, Caramelo JJ. 2005 Glycoprotein tertiary and quarternary structures are monitored by the same quality control mechanism. J Biol Chem. 2005;280:18138–41.

Kelleher, D. J. & Gilmore, R. 2006. An evolving view of the eukaryotic oligosaccharyltransferase Glycobiology, 16, 47R–62R.

Kemmink, J., Darby, N. J., Dijkstra, K., Nilges, M. & Creighton, T. E. 1996. Structure determination of the N-terminal thioredoxin-like domain of protein disulfide isomerase using multidimensional heteronuclear 13C/15N NMR spectroscopy Biochemistry, 35, 7684–7691.

Kimata Y, Ishiwata-Kimata Y, Ito T, Hirata A, Suzuki T, Oikawa D, Takeuchi M, Kohno K. 2007. Two regulatory steps of ER-stress sensor Ire1 involving its cluster formation and interaction with unfolded proteins. J Cell Biol. 2007;179:75–86.

Kincaid, M. M., and Cooper, A. A. 2007. Misfolded Proteins Traffic from the Endoplasmic Reticulum (ER) Due to ER Export Signals Mol. Biol. Cell 18 455–463.

Kitzmuller C., Caprini A., Moore S. E., Frenoy J. P., Schwaiger E., Kellermann O., Ivessa N. E., Ermonval M. 2003. Processing of N-linked glycans during endoplasmic-reticulum-associated degradation of a short-lived variant of ribophorin I. Biochem. J. 2003;376:687–696.

Kostova Z, Wolf DH. 2003. For whom the bell tolls: protein quality control of the endoplasmic reticulum and the ubiquitin-proteasome connection. EMBO J 22:2309–2317.

Lederkremer GZ. 2009. Glycoprotein folding, quality control and ER-associated degradation. Curr Opin Struct Biol. 2009 Oct;19(5):515-23. Epub 2009 Jul 17.

Lin JH, Li H, Yasumura D, Cohen HR, Zhang C, et al. 2007. IRE1 signaling affects cell fate during the unfolded protein response. Science. 2007;318:944–949.

Maattanen P., Kozlov G., Gehring K., Thomas D. Y. 2006. ERp57 and PDI: multifunctional protein disulfide isomerases with similar domain architectures but differing substrate-partner associations. Biochem. Cell Biol. 2006;84:881–889.

Meusser B, Hirsch C, Jarosch E, Sommer T. 2005. ERAD: the long road to destruction. Nat Cell Biol. 2005;7:766–772.

Nair, U. & Klionsky, D. J. 2005. Molecular mechanisms and regulation of specific and nonspecific autophagy pathways in yeast. J. Biol. Chem. 280, 41785–41788.

Nakatsukasa K., Brodsky J. L. 2008. The recognition and retrotranslocation of misfolded proteins from the endoplasmic reticulum. Traffic. 2008;9:861–870.

Ng, D. T., Spear, E. D. & Walter, P. 2000. The unfolded protein response regulates multiple aspects of secretory and membrane protein biogenesis and endoplasmic reticulum quality control. J. Cell Biol. 150, 77–88.

Oda Y, Hosokawa N, Wada I, Nagata K. 2003. EDEM as an acceptor of terminally misfolded glycoproteins released from calnexin. Science. 2003;299:1394–1397.

Palamarczyk G, Elbein AD. 1985. The effect of castanospermine on the oligosaccharide structures of glycoproteins from lymphoma cell lines. Biochem J. 1985 May 1;227(3):795–804.

R. Schekman and L. Orci. 1996. Coat proteins and vesicle budding. Science 271 (1996), pp. 1526–1533.

Rao, R. V., Ellerby, H. M. & Bredesen, D. E. 2004. Coupling endoplasmic reticulum stress to the cell death program. Cell Death Differ. 11, 372–380.

Ritter C, Helenius A. 2000. Recognition of local glycoprotein misfolding by the ER folding sensor UDP-glucose:glycoprotein glucosyltransferase. Nat Struct Biol. 2000;7: 278-280.

Ruddock, L.W., and M. Molinari. 2006. N-glycan processing in ER quality control. J. Cell Sci. 119:4373–4380.

Russell, S. J., Ruddock, L. W., Salo, K. E., Oliver, J. D., Roebuck, Q. P., Llewellyn, D. H., Roderick, H. L., Koivunen, P., Myllyharju, J., and High, S. 2004. The Primary Substrate Binding Site in the b′ Domain of ERp57 Is Adapted for Endoplasmic Reticulum Lectin Association*J. Biol. Chem. 279 18861-18869.

Schrag J. D., Bergeron J. J., Li Y., Borisova S., Hahn M., Thomas D. Y., Cygler M. 2001. The structure of calnexin, an ER chaperone involved in quality control of protein folding. Mol. Cell. 2001;8:633–644.

Schroder M, Kaufman RJ, 2005. The mammalian unfolded protein response. Annu Rev Biochem 2005, 74:739-89.

Schroder, M., and R.J. Kaufman. 2005. ER stress and the unfolded protein response. Mutat. Res. 569:29–63.

Sousa, M., and A.J. Parodi. 1995. The molecular basis for the recognition of misfolded glycoproteins by the UDP-Glc: glycoprotein glucosyltransferase. EMBO J. 14:4196–4203.

Stefano M. Marino and Vadim N. Gladyshev. 2008. A Structure-Based Approach for Detection of Thiol Oxidoreductases and Their Catalytic Redox-Active Cysteine Residues. Biochem Cell Biol. 2006 Dec;84(6):881-9.

Stigliano ID, Caramelo JJ, Labriola CA, Parodi AJ, D'Alessio C. 2009. Glucosidase II β Subunit Modulates N-Glycan Trimming in Fission Yeasts and Mammals. Mol Biol Cell. 2009 Sep;20(17):3974-84.

Taylor SC, Ferguson AD, Bergeron JJ, Thomas DY. 2004. The ER protein folding sensor UDP-glucose glycoprotein-glucosyltransferase modifies substrates distant to local changes in glycoprotein conformation. Nat Struct Mol Biol. 2004;11:128–134.

Taylor, S.C., A.D. Ferguson, J.J. Bergeron, and D.Y. Thomas. 2004. The ER protein folding sensor UDP-glucose glycoprotein-glucosyltransferase modifies substrates distant to local changes in glycoprotein conformation. Nat. Struct. Mol. Biol. 11:128–134.

Toby S. Scott-Ward and Margarida D. Amaral. 2009. Deletion of Phe508 in the first nucleotide-binding domain of the cystic fibrosis transmembrane conductance regulator increases its affinity for the heat shock cognate 70 chaperone. FEBS Journal. Volume 276 Issue 23, Pages 7097 – 7109.

Tokunaga, F., Brostrom, C., Koide, T., and Arvan, P. 2000. Endoplasmic reticulum (ER)-associated degradation of misfolded N-linked glycoproteins is suppressed upon inhibition of ER mannosidase I. J. Biol. Chem. 275 40757–40764.

Travers KJ, Patil CK, Wodicka L, Lockhart DJ, Weissman JS, Walter P. Functional and genomic analyses reveal an essential coordination between the unfolded protein response and ER-associated degradation. Cell. 2000;101:249–258.

Travers KJ, Patil CK, Wodicka L, Lockhart DJ, Weissman JS, Walter P. 2000. Functional and genomic analyses reveal an essential coordination between the unfolded protein response and ER-associated degradation. Cell. 2000;101:249–258.

Tsao YS, Ivessa NE, Adesnik M, Sabatini DD, Kreibich G. 1992. Carboxy terminally truncated forms of ribophorin I are degraded in preGolgi compartments by a calcium-dependent process. J Cell Biol. 1992; 116:57–67.

Varga K, Jurkuvenaite A, Wakefield J, Hong JS, Guimbellot JS, Venglarik CJ, Niraj A, Mazur M, Sorscher EJ, Collawn JF, Bebok Z. 2004. Efficient intracellular processing of the endogenous cystic fibrosis transmembrane conductance regulator in epithelial cell lines. J. Biol. Chem. 2004;279:22578–22584.

Vembar SS, Brodsky JL. 2008. One step at a time: endoplasmic reticulum-associated degradation. Nat Rev Mol Cell Biol. 2008;9:944–957.

Wada I, Imai S, Kai M, Sakane F, Kanoh H. 1995. Chaperone Function of Calreticulin When Expressed in the Endoplasmic Reticulum as the Membrane-anchored and Soluble Forms; J. Biol. Chem. 1995.270:20298–20304.

Williams, D.B. 2006. Beyond lectins: The calnexin/calreticulin chaperone system of the endoplasmic reticulum. J. Cell Sci. 119 615–623.

Wilson C, Farmery M, Bulleid N. 2000. Pivotal role of calnexin and mannose trimming in regulating the ER-associated degradation of MHC class I heavy chain. *J Biol Chem* 2000.

Wilson CM, Roebuck Q, High S. 2008.Ribophorin I regulates substrate delivery to the oligosaccharyltransferase core. Proc Natl Acad Sci USA. 2008;105(28):9534–9539.

Y. Wu, M.T. Swulius, K.W. Moremen and R.N. Sifers, 2003. Elucidation of the molecular logic by which misfolded alpha 1-antitrypsin is preferentially selected for degradation, *Proc Natl Acad Sci USA* 100 (2003), pp. 8229–8234.

Yuki H, Hamanaka R, Shinohara T, Sakai K, Watanabe M. 2005. A novel approach for N-glycosylation studies using detergent extracted microsomes. Mol Cell Biochem. 2005 Oct;278(1-2):157-63.

Yukiko Yoshida and Keiji Tanakaa. 2009. Lectin-like ERAD players in ER and cytosol. Biochimica et Biophysica Acta Vol. 1800, Issue 2, February 2010, Pages 172-180.

9. Appendix:

9.1. Abstract:

To ensure the integrity and fidelity of newly synthesized proteins, eukaryotic cells possess quality control (QC) mechanisms to monitor protein folding and assembly. The endoplasmic reticulum (ER) represents a key organelle for proteins destined for the secretory pathway and contains sophisticated proof-reading and elimination mechanisms. During maturation, many proteins targeted for the secretory pathway undergo N-glycosylation. The N-glycan (Glc3Man9GlcNAc2) is further processed by various sensor molecules that are able to discriminate between native and non-native protein conformations and covalently tag misfolded proteins. These proteins are recognized by the folding and degradation machinery including the unfolded protein response (UPR), the calnexin/calreticulin (CNX/CRT) cycle as well as ER-associated degradation (ERAD).

The aim of this study was to gain insight into the role of N-linked glycosylation, especially regarding the role of glucose residues in the N-linked glycan, during glycoprotein processing and degradation. Therefore, pulse-chase experiments with wild type (G3) and glycosylation-deficient Chinese hamster lung fibroblasts (QC) expressing either RI_{332} or its hemagglutinin (HA) epitope-tagged version, RI_{332}-6HA, were performed. RI_{332} and RI_{332}-6HA represent model substrates for aberrant proteins that interact with CNX/CRT and are substrates of the ERAD pathway. The mutant cells used in this study are glycosylation-deficient, i.e. they lack glucosylation of the N-glycan. Thus, aberrant proteins are not glucosylated in QC cells and might not enter the CNX/CRT cycle but be rapidly degraded.

Experiments performed to determine the degradation kinetics of RI_{332} or RI_{332}-6HA in G3 and QC cells surprisingly revealed that degradation of the model substrates is slowed in mutant cells compared to wild type cells, which might be due to their interaction with ER chaperones other than CNX or CRT.

Furthermore, pulse-chase experiments using inhibitors of proteasomal degradation such as ZLLL, and inhibitors of N-glycan processing, such as castanospermine, 1-deoxymannojirimycin (dMM) and kifunensine, were performed to gain insight into their influence on glycoprotein processing and degradation. Degradation of RI_{332} and RI_{332}-6HA was demonstrated to be proteasome-dependent, since inhibition with ZLLL led to stabilization of the model substrates. For experiments applying dMM and kifunensine, results were contradictory, but stabilization of RI_{332} and RI_{332}-6HA could be shown at least for G3 cells. Inhibition by castanospermine resulted in an increase of the half life of RI_{332} and RI_{332}-6HA in all clones except for G3 cells expressing RI_{332}. Thus, the role of the CNX/CRT cycle in the degradation of the ERAD model substrates in the glycosylation-deficient QC cells remains to be elucidated in further work.

9.2. Zusammenfassung:

Eukaryotische Zellen besitzen Qualitätskontrollmechanismen, die für die korrekte Faltung und den Zusammenbau von neusynthetisierten Proteinen sorgen. Ein wichtiges Zellorganell für die Proteine des sekretorischen Weges ist das endoplasmatische Retikulum (ER). Es besitzt ausgereifte Kontroll- und –Eliminationsmechanismen. Viele Proteine, die sich auf dem sekretorischen Weg befinden, werden N-glykosiliert. Das N-Glykan (Glc3Man9GlcNAc2) wird dann von verschiedenen Sensormolekülen, die in der Lage sind, zwischen nativen und nicht-nativen Proteinkonformationen zu unterscheiden, weiter prozessiert. Mechanismen wie die ungefaltete Proteinantwort (UPR), der Calnexin/Calreticulin (CNX/CRT) Zyklus sowie der ER-assoziierte Proteinabbau (ERAD) erkennen und verarbeiten diese Proteine weiter.

Das Ziel dieser Studie war es, einen Einblick in die Rolle der N-Glykosilierung von Glykoproteinen, speziell jener der Glukosilierung des N-Glykans, bei deren Verarbeitung und Abbau zu gewinnen. Dafür wurden Wildtyp (G3) und glykosilierungsdefekte Hamsterfibroblasten (QC), die entweder RI_{332} oder dessen Hämagglutinin (HA)-markierte Version, RI_{332}-6HA, stabil exprimieren, Pulse-Chase Experimenten unterzogen. RI_{332} und RI_{332}-6HA stellen Modellsubstrate für nicht-native Proteine dar. Sie interagieren mit dem CNX/CRT Zyklus und sind auch Substrate des ERAD. Den QC Zellen fehlt auf Grund einer Mutation die Glukosilierung der N-Glykane. Das führt dazu, dass nicht-native Proteine wie RI_{332} oder RI_{332}-6HA nicht glukosiliert werden, vermutlich nicht mit CNX/CRT interagieren können und daher schneller abgebaut werden. Somit stellten G3 und QC Zellen, die RI_{332} und RI_{332}-6HA stabil exprimieren, die idealen Zellmodelle dar, um die Rolle der Glukosilierung bei der Verarbeitung und dem Abbau von Glykoproteinen zu studieren. Überraschenderweise zeigten Versuche, die zur Bestimmung der Abbaukinetik von RI_{332} oder RI_{332}-6HA in G3 und QC Zellen durchgeführt wurden, eine Stabilisierung der Modellproteine in den QC Zellen, die auf einer Interaktion von RI_{332} und RI_{332}-6HA mit anderen ER-Chaperonen basieren könnte.

Weiters wurden Pulse-Chase Experimente unter Verwendung von Inhibitoren des Proteasomabbaus (ZLLL) und Inhibitoren der N-Glykanverarbeitung wie Castanospermin, dMM (1-deoxymannojirimycin) und Kifunensin durchgeführt, um deren Auswirkungen auf die Glykoproteinverarbeitung und -abbau zu erforschen. Wie erwartet, wurden die Modellproteine durch Inhibierung mit ZLLL stabilisiert. Die Ergebnisse von den Versuchen mit dMM und Kifunensin waren nicht ganz eindeutig, eine Stabilisierung von RI_{332} und RI_{332}-6HA konnte aber für G3 Zellen gezeigt werden. Experimente mit Castanospermin führten auch zu einer Verlängerung der Halbwertszeit von RI_{332} oder RI_{332}-6HA, die RI_{332}-exprimierenden G3 Zellen ausgenommen. Somit bleibt es weiterführenden Experimenten vorbehalten, die Rolle des CNX/CRT Zyklus im Abbau von ERAD Substraten in der Glykosilierung-defizienten QC Zelllinie zu klären.

9.3. Curriculum Vitae:

Angaben zur Person

Name	**Johanna Levy, geb. Parson**
Adresse	Lindengasse 22/ 17 1070 Wien
Telefon	0650/7758811
E-Mail	**johanna_parson@gmx.at**
Staatsangehörigkeit	Österreich
Geburtsdatum	30.01.1984

Ausbildungsweg

10/2003-dato	Studium der Molekularen Biologie, Universität Wien Schwerpunktsfächer: Mikrobiologie/ Immunologie, Zellbiologie, Neurobiologie
10/ 2002-09/2003	Studium der Biologie, Universität Innsbruck
09/1994-06/2002	Bundesrealgymnasium Adolf-Pichler-Platz, Innsbruck

Arbeitserfahrung

03/2009-11/2009	Diplomarbeit, Labor Ao. Univ.-Prof. DI Dr. N. Erwin Ivessa, Institut für medizinische Biochemie, Abteilung Molekulare Genetik, Medizinische Universität Wien
10/2008-11/2008	Wahlbeispiel Labor M.Jantsch
06/2007	Wahlbeispiel Labor Hilberg, Boehringer Ingelheim RCV
02/2007-03/2007	Wahlbeispiel Labor Charpentier
2003-07/200306/	Praktikum bei Infineon Technologies, München; Entwicklung von DNA-Mikrochips

Sprachen

Muttersprache	Deutsch
Fremdsprachen	Englisch, Französisch, Spanisch